A SAND-FILLED MEANDERING CHANNEL, UPPER HORSESHOE CANYON FORMATION (UPPER CRETACEOUS), DRUMHELLER, ALBERTA.

A SAND-FILLED MEANDERING CHANNEL, UPPER-HORSESHOE CANYON FORMATION (UPPER-CRETACEOUS), DRUMHELLER, ALBERTA.

BY

SUZANNE ELIZABETH PAGANI

A Thesis Submitted To The Department Of Geology

In Partial Fulfillment Of The Requirements For

The Degree Of Bachelor Of Science.

McMaster University

1985

BACHELOR OF SCIENCE (1985) McMASTER UNIVERSITY

Hamilton, Ontario

TITLE: A Sand-Filled Meandering Channel, Upper Horseshoe Canyon Formation (Upper Cretaceous), Drumheller, Alberta.

AUTHOR: Suzanne Elizabeth Pagani

SUPERVISOR: Dr. R.G. Walker

NUMBER OF PAGES: xiii, 100

ABSTRACT

Three fluvial channels of the Upper Cretaceous Horseshoe Canyon Formation are exposed at Drumheller Alberta. The channels are isolated lenticular bodies and are separated by abundant fine-grained sediment.

One channel appears to be filled to the top with sand and contains large, concave upward surfaces. The other channels contain well defined lateral accretion surfaces and large scale trough cross-bedding. Associated with the channel sands are levee, crevasse splay and distal overbank deposits. These channels are interpreted as high sinuosity, suspended load, meandering channels.

Paleoflow directions measured in the cross-bedded sands indicate paleoflow directions towards the east.

Grain size distribution plots for the sandstones commonly lack a coarse population of grains transported by traction. Flow calcuations show that the channels were competent to move grain sizes much larger than those present within the channels. This leads to the conclusion that the characteristics of the traction population were strongly dependant on the supply of coarse material. Shear velocities in the channels were calulated to range from 3.1 to 9 cm s^{-1}.

The proposeed mechanism for the sand filling of a meandering channel is through gradual abandonment by chute cutoff. Maintenance of flow conditions, capable of

transporting sand, due to the decrease of depth with discharge, allowed the continued deposition of sand within the channel. Evidence of scoured surfaces within the channel indicate that any fines that may have been deposited were eroded away during flood stages when the meander loop was reoccupied.

ACKNOWLEDGEMENTS

I would like to thank Dr. R.G. Walker for suggesting the topic and for his supervision and advice.

The field work for this thesis would have been impossible without the expert guidance of Greg Nadon and the help of my friends, Ceri, Holly, and Dave. Kathy Bergman deserves special thanks for spending a grueling seven consecutive days assisting in the field and for keeping my spirits up when I was ready to quit and head for the nearest bar.

Dr. Guy Plint provided much needed encouragement and advice. Dave Collins helped in the grain size analysis methods and interpretation.

Jack Whorlwood's expert touch with regards to the photographic work was greatly appreciated. I would also like to thank Len Zwicker for preparing the thin sections.

Special thanks go to Dan, who, when the crunch was on, did much of the typing. I would also like to thank him for all his support and understanding, without which, this thesis would not have been possible.

TABLE OF CONTENTS

LIST OF FIGURES

LIST OF TABLES

CHAPTER 1

1.1 The Problem of Sand-Filled Channels:

Excellent outcrops of fluvial channels are present north of the city of Drumheller in the strata of the Upper Horseshoe Canyon Formation of the Edmonton Group. The area is often a stop for geological field trips and a photograph of one of the channels is included in the A.S.P.G. Ninth Annual Field Conference guidebook (1959).

One of the channels is unusual because it appears to be entirely sand filled. In meandering channels, sand is normally deposited in fluvial channels during their active stage, onto lateral accretion surfaces. The channel fills when it is either abandoned by the stream or undergoes a gradual decrease in flow due to reduction of depth and slope; the fill usually consists of a plug of fine material. In the case of abandonment, as in chute or neck cutoffs, the abandonded meander loop is filled by a plug of fines introduced by overbank from the active portion of the stream. In the case of gradual flow reduction, competence gradually decreases, resulting in the deposition of fines as channel fill. In contrast to meandering systems, braided channels fill to the top with sand by vertical accretion and do not contain a clay plug. Braided channel deposits

consist of laterally extensive sheets of sand and are not confined by clay plugs.

The sand filled channel and the other paleochannels in the area consist of isolated, lenticular sand bodies surrounded by abundant, fine-grained sediment. The sand body geometry more closely resembles deposits of a meandering channel deposit, therefore creating the problem of how meandering channels can fill to the top with sand. The purpose of this study is to propose possible explanations for the sand filling of the channel.

Field work in this study included measuring sections through the three channel outcrops, and paleocurrent determinations. The associated lab work involved grain size determination and petrography as well as an attempt at paleo-reconstruction of the channel(s).

1.2 Location and Accessibility:

Excellent and continuous exposures of flat-lying clastic rocks of Upper Cretaceous and Paleogene age are present along the Red Deer River Valley of the central Alberta badlands. The strata exposed along the valley walls comprise the shallow marine Bearpaw Formation of the Campanian Stage, the deltaic and fluvial Edmonton Group of the Campanian to Maestrichtian Stages and the continental Paskapoo Formation. Due to the presence of almost 100% outcrop, these exposures, especially the deltaic facies of

the lower Edmonton Group, are of interest because lateral facies relationships are easily studied.

The study area is located less than 1 km north of Drumheller in an abandoned river valley that is now occupied by Highway 9 (fig. 1.1). Drumheller is approximately 120 km northeast of Calgary. Two of the channel outcrops are easily visible from the road in the valley walls east of the highway. A small, unpaved parking area is located at the base of the outcrop, making it easily accessible by car. The channels can be reached by a 25 m climb up the valley side.

Weather is an important factor in the accessibility of the outcrops. The presence of bentonite clays makes field work difficult to impossible in wet weather. The sand bodies and surrounding lithologies pose several problems due to poor consolidation in the rocks. Although lateral continuity is good in most places, in some areas slumping obscures parts of the outcrops. Surface weathering has obliterated many of the sedimentary structures in the sand except in areas where "coffee grounds" drape bedding surfaces or where preferential cementation has occurred in the hoodoos.

Figure 1.1: Location of study area.

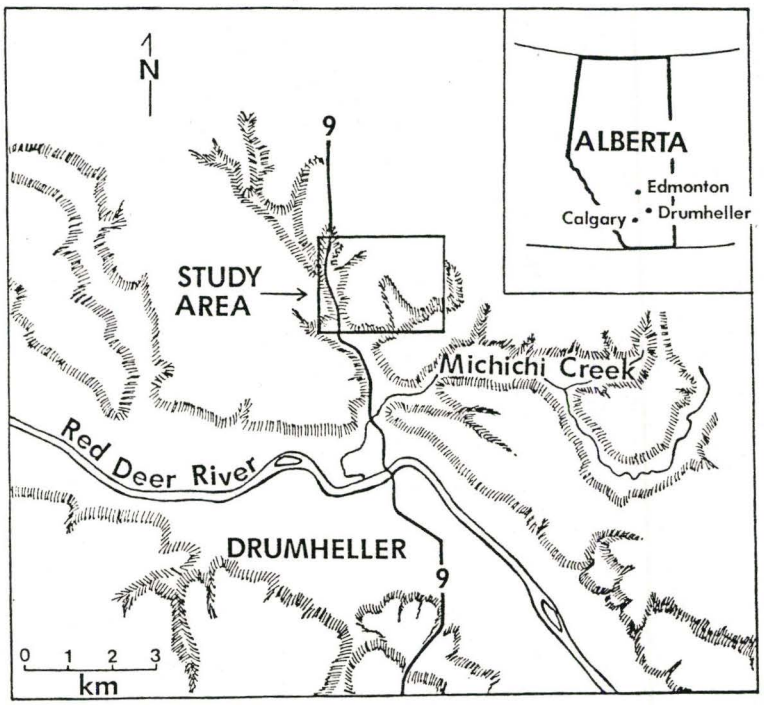
N
9
ALBERTA
Edmonton
Calgary
Drumheller
STUDY
AREA
Michichi Creek
Red Deer River
DRUMHELLER
9
0 1 2 3
km

1.3 Local Stratigraphy:

In east central and southern Alberta, the Upper Cretaceous Bearpaw Formation and Edmonton Group are exposed in an arc-shaped belt approximately 500 miles long and 60 miles wide (fig. 1.2).

The Bearpaw comprises up to 360 m of dark grey to brown-grey marine clays, shales and silty shales.

The Edmonton Group conformably overlies the Bearpaw shale and consists of deltaic and fluvial sediments. The Edmonton Group has undergone many previous subdivisions, which have been summarized by Irish (1970). In a 1968 paper he extended the names Whitemud and Battle Formations from southeast Alberta to their equivalents in the Edmonton "Formation" of the Oldman River -- Red Deer River region. In the previously mentioned 1970 paper he redefined the Edmonton "Formation" as a group. He proposed that the Edmonton Group be divided into three formations, the Horseshoe Canyon, the Whitemud and the Battle Formations. The Horseshoe Canyon Formation is described as consisting of interlensed bentonitic, argillaceous sandstones, bentonitic shales and coal seams. The Whitemud is defined as the white weathering, green-grey, argillaceous sandstone and light grey clay and the Battle Formation as massive, grey-weathering, purplish black bentonitic shale. Within the Battle Formation is the Kneehills Tuff, a dark bentonitic shale. It is believed to represent contemporaneous

Figure 1.2: The Upper Cretaceous Edmonton Group outcrops in an arc-shaped belt in east-central and southern Alberta. (From Irish, 1970)

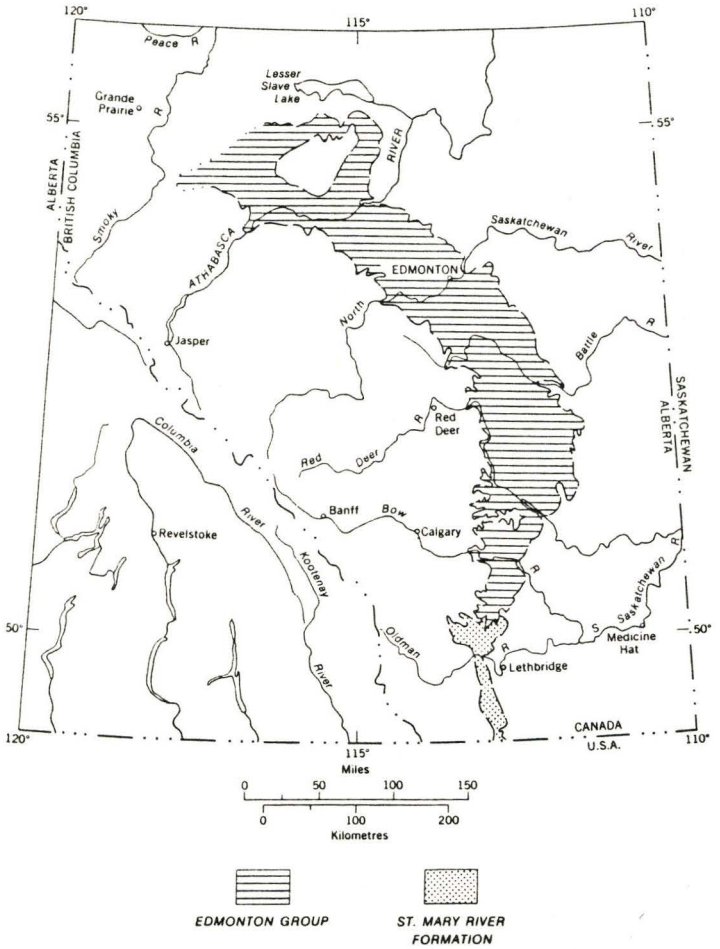
120°
115°
110°
55°
50°
Peace R.
Grande Prairie
Lesser Slave Lake
RIVER
ALBERTA
BRITISH COLUMBIA
Smoky R.
ATHABASCA
Saskatchewan River
EDMONTON
North
Battle R.
Jasper
Red Deer R.
Red Deer
SASKATCHEWAN
ALBERTA
Columbia River
Banff
Bow R.
Calgary
Revelstoke
Kootenay R.
Oldman R.
Saskatchewan R. S.
Medicine Hat
Lethbridge
CANADA
U.S.A.
Miles
0 50 100 150
0 100 200
Kilometres
EDMONTON GROUP
ST. MARY RIVER FORMATION

deposition of wind transported volcanic ash and is therefore considered an excellent time marker. Carrigy (1970) revised the boundaries between the Edmonton Group and the overlying Paskapoo Formation, placing the contact at the top of the Kneehills Member of the Battle Formation.

Equivalents to the Edmonton Formation are present in the foothills where the Bearpaw shale wedges out and the Edmonton combines with the Belly River Formation to form the Brazeau Formation. In north-western Montana and the south-western Alberta Foothills, Edmonton age strata are known as the St. Mary's River Formation and in the north-western Alberta Plains and Foothills as the upper portion of the Wapiti Formation (Table 1.1).

1.4 Biostratigraphy:

Since the Edmonton Group is non-marine, the best estimates regarding age of the group have been done on the basis of dinosaurian remains. With the retreat of the Cretaceous Seaway southward, the youngest Cretaceous marine sediments in the Canadian Western Interior contain the *Baculites grandis* zone and are only Maestrichtian in age.

The Late Maestrichtian deposits are characterized by dinosaurian fauna, such as *Triceratops*, *Tyrannosaurus* (fig. 1.3), *Thescelosaurus* and *Ankylosaurus*. *Triceratops* remains are most commonly used in dating the Edmonton Group. *Triceratops* is confined to the Upper Edmonton beds and its latest appearance marks the Cretaceous-Tertiary boundary.

Table 1.1: Formations of Alberta.

(Adapted from Williams and Burk,

1964, and Irish, 1970)

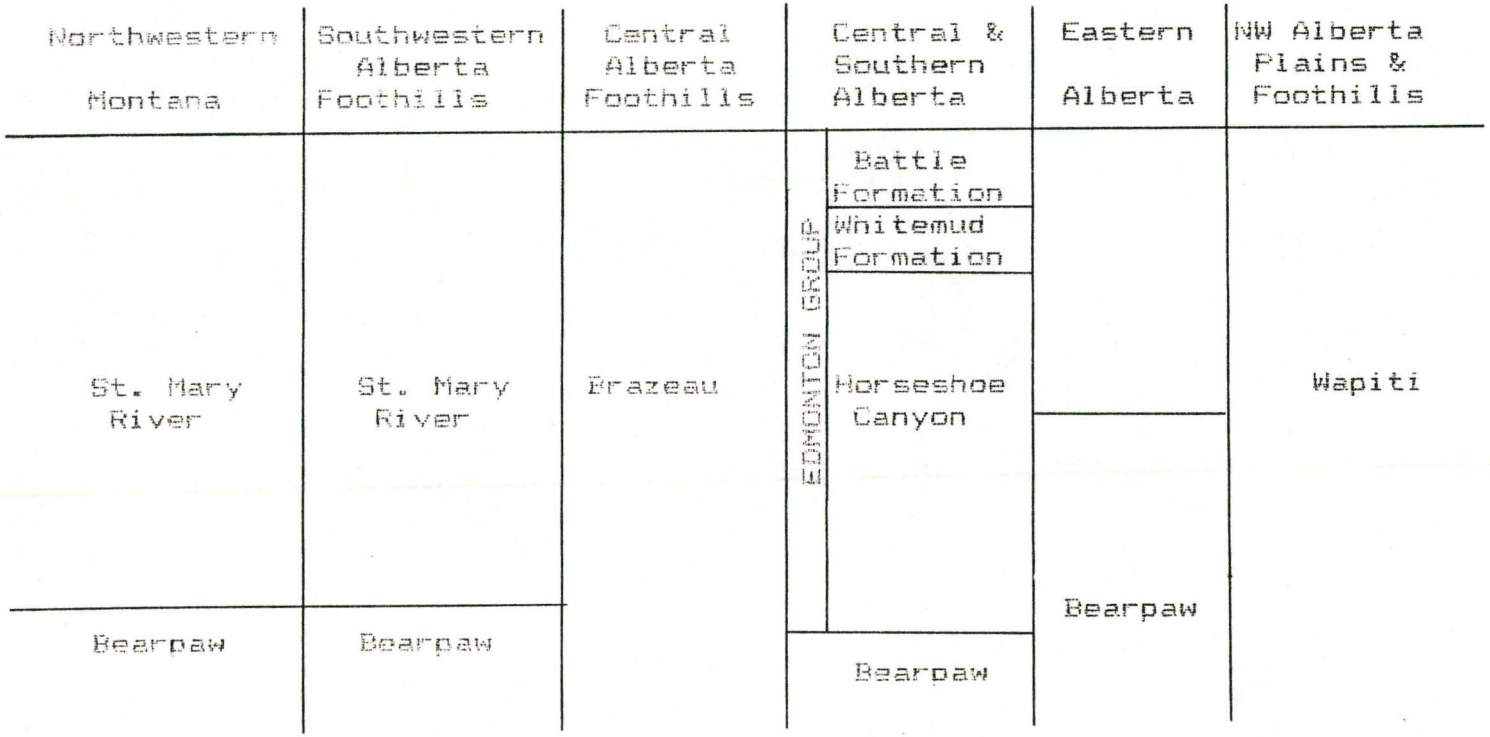
Northwestern Montana
Southwestern Alberta Foothills
Central Alberta Foothills
Central & Southern Alberta
Eastern Alberta
NW Alberta Plains & Foothills
EDMONTON GROUP
Battle Formation
Whitemud Formation
Horseshoe Canyon
St. Mary River
St. Mary River
Brazeau
Wapiti
Bearpaw
Bearpaw
Bearpaw
Bearpaw

Based on the radiometric ages of the Kneehills Tuff, which lies below the interval containing the dinosaur remains, and a bentonite bed, which lies above the Triceratops zone, the Cretaceous-Tertiary boundary has been dated at 64 to 65 million years b.p. (Obradovich and Cobban, 1975). The Triceratops beds of the Edmonton Group can be correlated with the Lance, Hell Creek and Frenchman Formations of Wyoming, Montana and Cypress Hills, Saskatchewan (Tozer, 1956).

1.5 Geologic History:

A broad epieric sea covered the Western Canadian Interior during late Cretaceous times. The sea was bounded to the west by the uprising Cordillera and by the Canadian Shield to the east. To the north and south, the seaway was open, connected to the Arctic Ocean and Gulf of Mexico respectively.

A northwesterly transgression of the sea during the Campanian Stage resulted in the deposition of the Bearpaw shale, after which tectonic activity in the area increased significantly. This created an abundant supply of clastic sediments, which built up and caused a movement of the shoreline to the east, allowing the accumulation of the continental Edmonton Group and its equivalents. (Williams and Burk, 1964)

Figure 1.3: The carnivorous Tyrannosaurus Rex prepares to devour a sedimentologist.

Figure 1.4: Fault in the strata of the upper horseshoe Canyon Formation. The throw on the fault is approximately 50 feet, and is visible by the displacement of the coal. Note the lateral continuity of the coal seam.

1.3

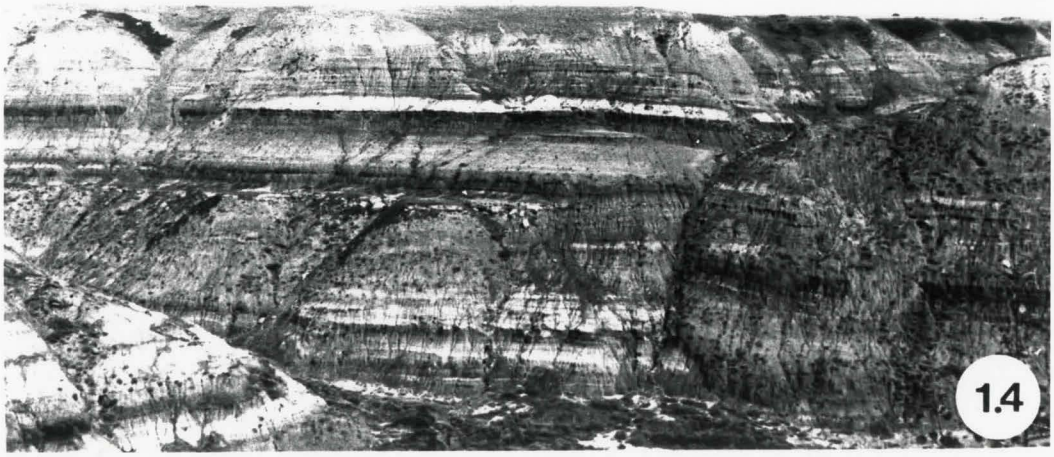

1.4

1.6 Structure:

The Upper Cretaceous sediments in the Alberta Plains region have undergone very little structural deformation. The strata are relatively flat lying, dipping west at a very low angle into the Alberta Syncline.

The strata in the Drumheller area contain several very gentle flexures trending north-west. The coal beds show anticlinal folds with widths ranging from less than one to tens of metres and heights on the order of 3 m. The folds have been attributed to the uneven settling of the coal beds during compaction (Irish, 1967).

Small faults have been found in the subsurface but the only surface outcrop of a fault exists in the study area (fig. 1.4). The fault strikes 050 and dips south-east at an angle of 80 degrees.

1.7 Previous Work:

Previous studies of the Edmonton Group (Irish, 1968,1970 and Carrigy, 1970) have involved changes in nomenclature and redefinition of formation boundaries (discussed in Chapter 1.3). A thorough review of previous literature on the Edmonton Group is contained in the 1970 paper by Irish.

Much of the recent work in the Drumheller area involves the transition zone between the marine Bearpaw Formation and the continental Edmonton Group. The first detailed work was conducted by Shepheard and Hills (1970) who interpreted the depositional environment of the transition zone as an

easterly prograding deltaic complex and compared it to a river dominated delta such the Mississippi Delta. Rahmani (1983) agreed with the general depositional model that Shepheard and Hills proposed but interpreted the strata as an example of a wave dominated delta (c.f. the Rhone Delta). In his studies of the transition zone, Rahmani (1982), interpreted a record of four shoreline transgressions followed by barrier island progradations in the underlying Bearpaw Formation. These events marked the final stages of the Bearpaw marine transgression.

The sedimentology of the Horseshoe Canyon Formation has been examined in the subsurface near Red Deer, Alberta, by Rahmani and Nurkowski (1982), resulting in an informal division of the formation into two units. The lower fine-grained unit was intrepreted as being deposited in a lacustrine environment and the upper coal-bearing unit as accumulating in a meandering fluvial system.

A heavy mineral analysis on Upper Cretaceous and Paleocene sandstones in Alberta and adjacent areas of Saskatchewan revealed a distribution of heavy minerals that suggested a dominantly south-east flowing fluvial system (Rahmani and Lerbekmo, 1973).

The coal bearing unit of Rahmani and Nurkowski (1982) was studied in subsurface and in outcrop by Waheed (1983), who interpreted the lower Horseshoe Canyon Formation as delta plain environment and the upper part of the formation as representing deposition in diverse fluvial environments,

including those of meandering channels. The coal seams in the Horseshoe Canyon Formation were determined to occur in three environments; channel margin swamps, channel-fill swamps and back-barrier swamps. The general paleoflow direction of the Horseshoe Canyon was determined to be towards the east and a western igneous-sedimentary source of sediments was suggested.

CHAPTER 2

FACIES DESCRIPTIONS

The channels and the associated underlying, overlying and laterally adjacent strata have been divided into eight facies on the basis of lithology, sedimentary structures, clast content and sand:shale ratios. Brief interpretations are included with each of the facies descriptions and an integrated facies interpretation will be presented in Chapter 8. Positions of the facies with respect to one another and their integration into the channel environment as a whole are illustrated and discussed in Chapter 3.

2.1 Facies 1: Coal

The coal facies comprises one laterally continuous coal bed, 2 to 2.4 m thick, which constitutes a regional marker (fig. 1.4). The contact with the overlying facies is sharp and the lower contact is gradational.

The coal is low grade and friable and contains plant remains, small particles of amber and large (.3 m x .1m), well preserved, silicified wood fragments (fig. 2.1). It is vertically jointed, the joints striking at 060 (fig. 2.2).

Interpretation:

Coal deposits generally form in wet, highly vegetated areas such as on river floodplains or in coastal marshes (Miall, 1981). Because of the fluvial nature of the

Figure 2.1 Silicified log in coal.

Figure 2.2 Vertical jointing in coal.

2.1

2.2

underlying and overlying sediments, the coal can be interpreted as forming in a poorly-drained fluvial floodplain environment.

2.2 Facies 2: Interbedded Sand/Shale Facies

The interbedded sand/shale facies is composed of parallel laminated sand interbedded with shale. The sand interbeds range from .20 to .75 m in thickness, with individual laminae 1 cm in thickness. The shale ranges from .10 to .25 m in thickness and the sand to shale ratio is approximately 4:1. The maximum thickness of this facies is 2 m. Both the upper and lower contacts are sharp.

The sand body is wedge-shaped and contains low angle (6 degrees), westerly dipping surfaces that are defined by a coating of "coffee grounds" (finely comminuted plant debris) and by siderite staining. These surfaces do not truncate any bedding planes and are themselves truncated by several concave upwards scours at the base of the overlying sand.

Convolute laminations are present in the sands (fig. 2.3). Well rounded, grey mudclasts and coalified plant clasts with associated amber are present in the bottom of this facies.

This facies is present only in Channel 1.

Figure 2.3 Convolute laminations in the sand of Facies 2.

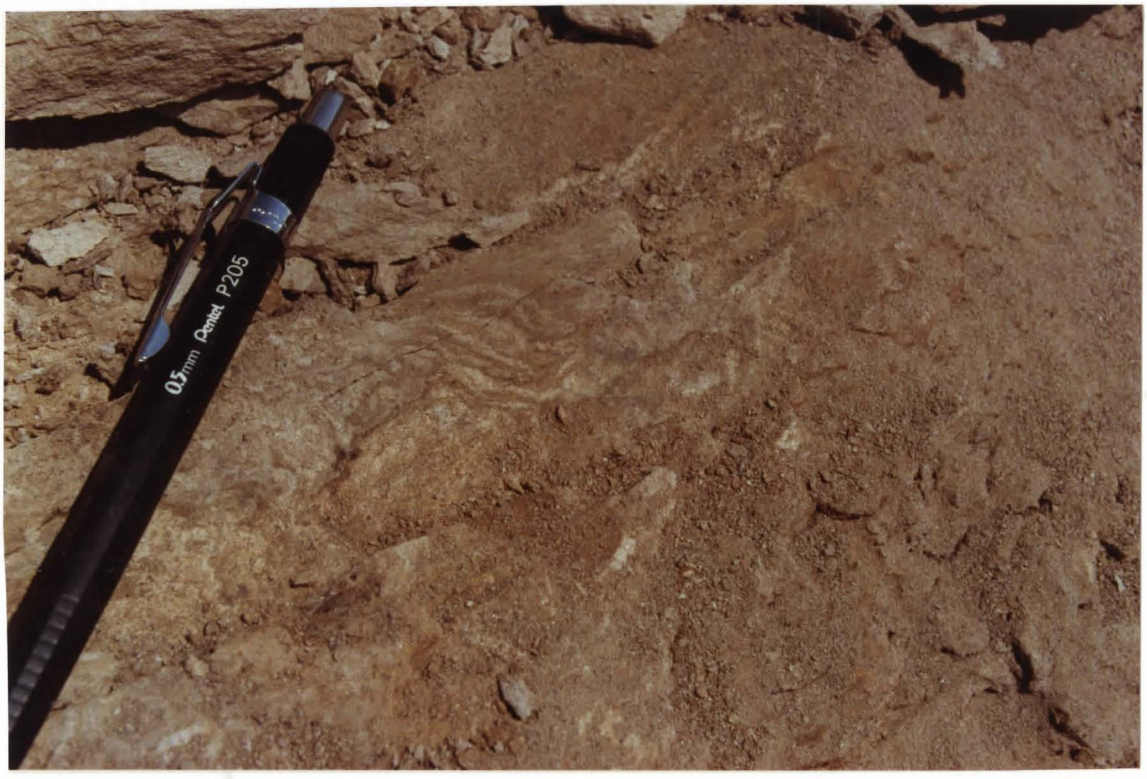
0.5mm Pentel P205

Interpretation:

The presence of low angle dipping surfaces coated with mud layers and coffee grounds could suggest deposition on the point bar of a meandering channel.

The shale interbeds may have been deposited during periods of lower flow and indicate that poiint bar growth was highly discontinuous (Puidefabregas and Van Vliet, 1978). The convolute laminations may be due to rapid deposition of the mud drapes resulting in an increase in pore pressure in the sand causing liquefaction and plastic deformation (Collinson and Thompson, 1982).

2.3 Facies 3: Clast-rich Sand

This facies consists of .3 to .8 m thick sand lenses which extend along the entire lower boundary of Facies 5. The lower contact of this facies is erosive and the upper contact is gradational.

As the name implies, the major feature of this sand is the presence of abundant organic debris and mudclasts. The organic debris occurs as large and fine grained coalified wood and plant fragments (figs. 2.4 and 2.5). The mudclasts have two forms; small, grey spherical to ovoid clasts which range in size from .5 to 1 cm and large tabular mudclasts with lengths of up to .20 m. The tabular mudclasts show preserved fine lamination as well as evidence of plastic deformation (fig. 2.6). These mudclasts may have been derived from Facies 8.

Figure 2.4 Coalified plant fragments found in Facies 3.

Figure 2.5 Coal clasts in Facies 3.

Figure 2.6 Large tabular mudclast as indicated by arrows.

Figure 2.7 Leaf impressions on bedding surfaces of shale in Facies 4.


6
5
4
3
2
1
2.6

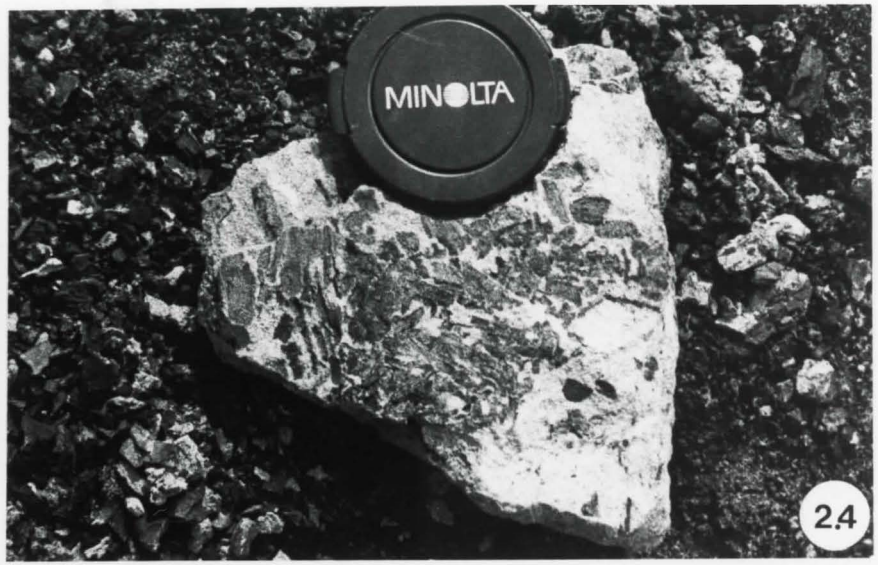
MINOLTA
2.4

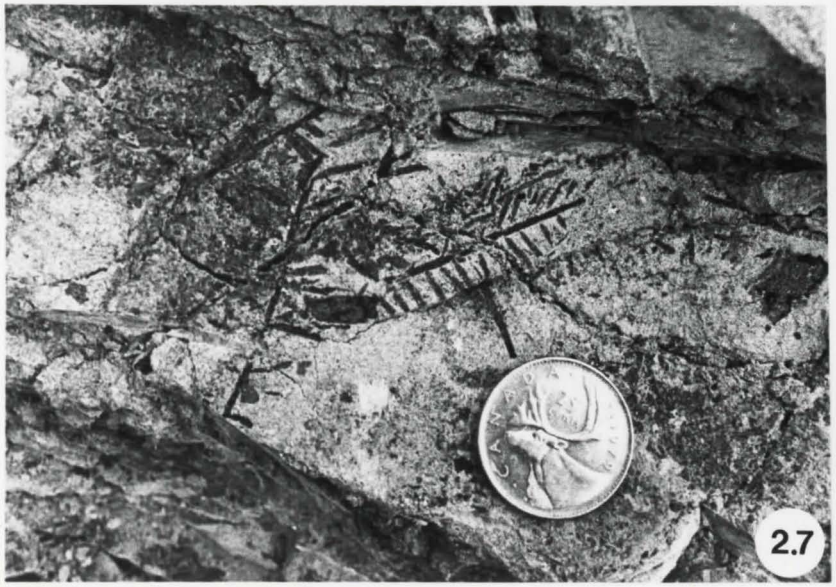
2.7


2.5

Due to weathering of the outcrop face, sedimentary structures in this sand are not visible.

Interpretation:

This facies is interpreted as deposited during periods of high flow due to the abundance of very coarse materials such as mudclasts and coalified plant fragments, and the presence of an erosional base.

2.4 Facies 4: Interfingering Brown Shale and Sand

This facies comprises .3 to 1.5 m thick lenses of finely laminated fissile brown shale interfingering with sand lenses which range in thickness from .3 m to 1.4 m, giving a sand to shale ratio of approximately 1:1. The upper and lower contacts of this facies are sharp. Contacts between the shale and sand within the facies are also sharp.

The lamination thickness in the shale decreases systematically upwards from .6 cm to .2 cm in each unit. Fine coalified plant fragments are homogeneously distributed throughout the shale. Yellow, rounded mudclasts are present but not abundant.

The interfingering sand bodies have convex upward tops and tend to pinch out laterally. The sand contains rounded mudclasts as well as abundant coalified plant fragments. On bedding surfaces in the shale and on the lower bedding surfaces in the sand, leaf impressions occur singly or as mats of leaves (figs. 2.7 and 2.8).

This facies is present only in Channel 1.

Figure 2.8 Impression of mat of leaves on bedding surfaces of the sand in Facies 4.


0.5mm Pentel P205

Interpretation:

The interfingering brown shale and sand represents an environment of organic rich mud accumulation. The presence of mud indicates periods of quiet deposition followed by catastrophic sand deposition as indicated by the erosional contacts between the sand and shale and the clasts present in the sand.

The brown colouration of the shale is a result of oxidation of iron bearing minerals and could indicate subaerial exposure with periodic wetting (Allen, 1965).

2.5 Facies Sa: Cross-Bedded Sand With Low Angle Dipping Surfaces

The cross-bedded sand bodies range in thickness from 3 to 4 m and have lateral extents of 49 to more than 84 m Their shapes range from tabular to lenticular. Contacts with the underlying and overlying facies are gradational.

Large scale sedimentary structures include trough cross-bedding and low angle dipping surfaces which may be interpreted as lateral accretion surfaces. The troughs have widths ranging from .5 to 1.5 m (fig. 2.9). Individual beds are on the order of 2 to 3 cm in thickness and sets range from 8 to 15 cm in thickness (fig. 2.10). The lateral accretion surfaces are on the scale of 7.1 to 25 m in length and dip at an average angle of 8 degrees.

Figure 2.9 Large scale trough cross-beds in Facies 5a. Note the truncation of one trough by another. (scale bar=1 m)

Figure 2.10 Individual beds in trough cross-bedding of Channel 2. (Dinosaur is 15 cm in length)

Figure 2.11 A coating of "coffee grounds" define the bedding surfaces in Facies 5.

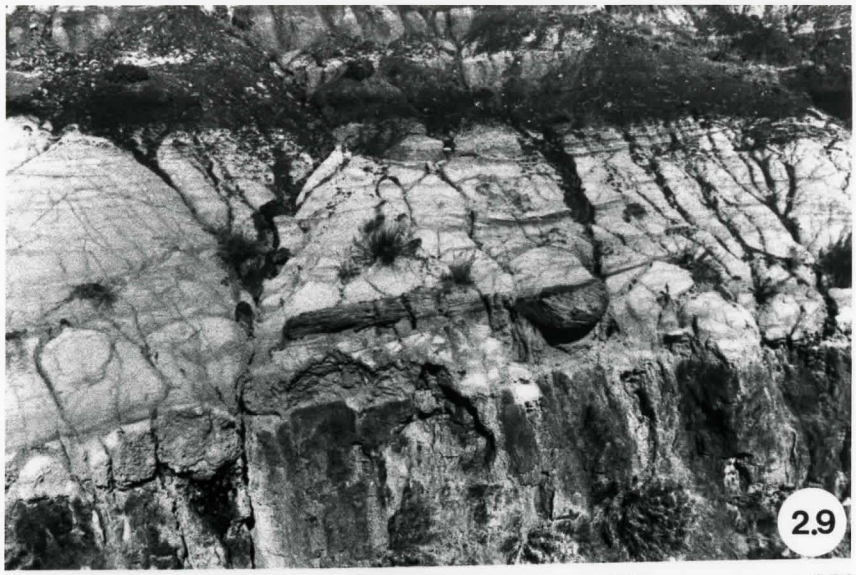

2.9

2.10

2.11

The troughs and lateral accretion surfaces are defined by "coffee grounds" coating the bedding surfaces (fig. 2.11), as well as by siderite staining.

Ripple cross-lamination is visible only where the sediments are lithified and form hoodoos and appears to be superimposed on the larger scale sedimentary structures. Individual laminae are on the millimetre scale in thickness and set thicknesses are from 1.5 to 2.5 cm.

Interpretation:

The association of lateral accretion surfaces with trough cross-bedded sand suggests deposition on a point bar surface in a meandering channel. The large scale trough cross-oed can be attributed to the migration of sinuous-crested dunes within the channel and are indicative of lower flow regime (Collinson and Thompson, 1982). The coatings of "coffee grounds" on the bedding surfaces may indicate episodic deposition of fine material.

2.6 Facies 5b: Cross-Bedded Sand

The primary difference between the sand of this sub-facies and that of Subfacies 5a is the absence of the prominent low angle dipping surfaces in 5b. Instead the sand contains large scale, concave upward surfaces with coffee grounds coating bedding surfaces (figs. 2.12 and 2.13). Trough cross-bedding is also present in this facies.

Figure 2.12 Large, concave-upward surfaces are present in Facies 5b. Note the absence of lateral accretion surfaces. (Sand body width is 4.7 m).

Figure 2.13 The lower portion of Facies 5b in Channel 1 shows an abundance of "coffee grounds" coating the bedding surfaces.

Figure 2.14 Rib and furrow structure preserved in hoodoo indicates paleoflow direction of 070.

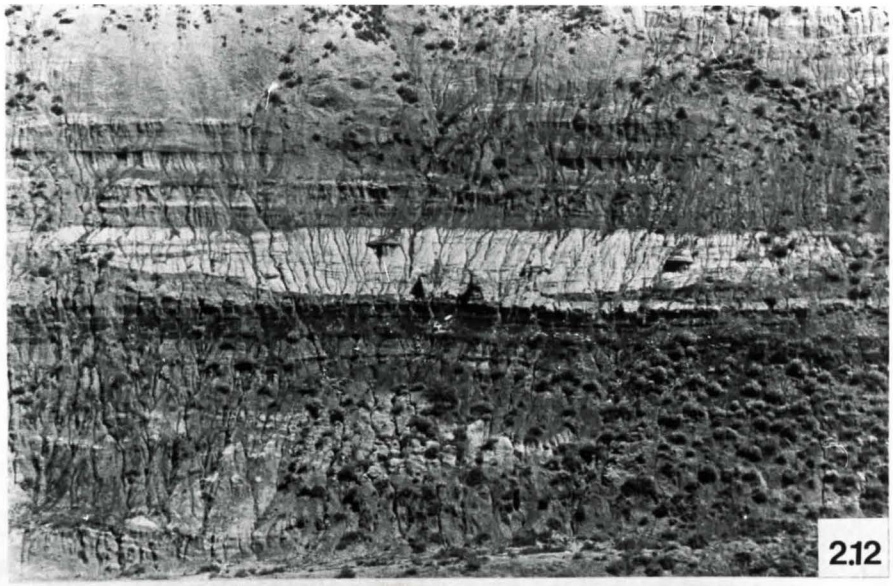

2.12

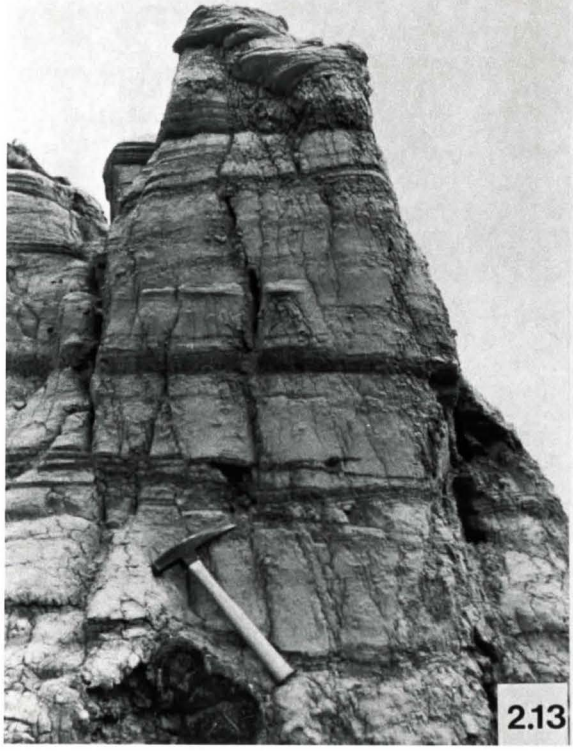

2.13

2.14

The overall shape of this sand body is concave upward with a flat top. The maximum thickness of the sand is 4.7 m and it has an approximate cross-sectional width of 43.6 m.

The abundance of coffee grounds coating the bedding surfaces decreases upward in this facies.

Interpretation:

Gently dipping, concave upward surfaces associated with trough cross-bedding and ripple cross-lamination can be interpreted as resulting from dune migration with periods ofscouring.

2.7 Facies 6: Finely Laminated Sand

The 10 to 15 cm finely laminated sand facies are found directly above and within the cross-bedded sand. The upper contact of this facies may be sharp or gradational and the lower contact is gradational.

The only sedimentary structure observed is parallel lamination, defined by parting lineation, with laminae thickness of approximately .5 cm (fig. 2.15).

The bedding surfaces are coated with "coffee grounds" and larger coalified plant clasts.

Interpretation:

The presence of finely laminated sand is attributed to flows with high velocities and shallow depths and is interpreted as upper flat-bed.

2.8 Facies 7: Carbonaceous Shale

The carbonaceous shale is bounded by a sharp lower contact and commonly a gradational, but occasionally erosive, upper contact. It has an average thickess of .3 m but can have thicknesses up to 1.5 m.

This facies consists of red, friable shale with a high concentration of fine coaly material and larger coalified plant fragments. The abundance of coaly material increases upward resulting in a darkening in colour towards the top of this facies (fig. 2.16).

This facies most commonly occurs directly above the channel sands.

Interpretation:

The carbonaceous shale was deposited in a quiet environment where organic detritus was in abundant supply. The red colouration of the sediment can be attributed to exposure in a warm dry environment with periodic wetting (Buurman, 1975).

2.9 Facies 8: Grey Shale

This facies consists of a grey, friable shale (fig. 2.17) with beds approximately 1 m in thickness interbedded with sand stringers 10 to 20 cm thick with a shale to sand ratio of 10:1. The total thickness ranges from 2.8 to 3.5 m. The sand stringers appeared to be roughly flat lying (fig. 2.18) although weathering and poor accessibility prevented detailed work on this facies.

Figure 2.15 Finely laminated sand. Note the parting lineation which is emphasized by coalified particles coating bedding surfaces.

Figure 2.16 Carbonaceous shale (Facies 7).

Figure 2.17 Finely laminated, friable grey shale of Facies 8.

Figure 2.18 Thin sand stringers present in Facies 8 below Channel 3.

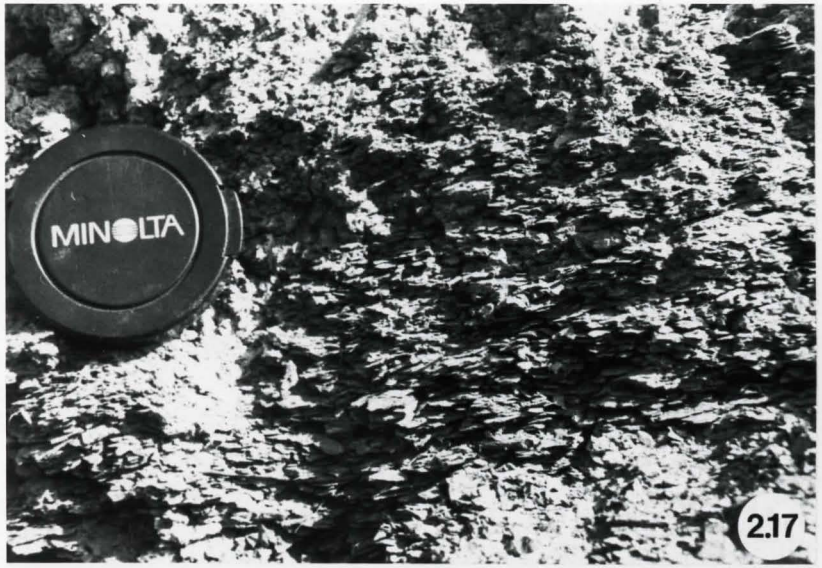
MINOLTA
2.17


MINOLTA
2.15

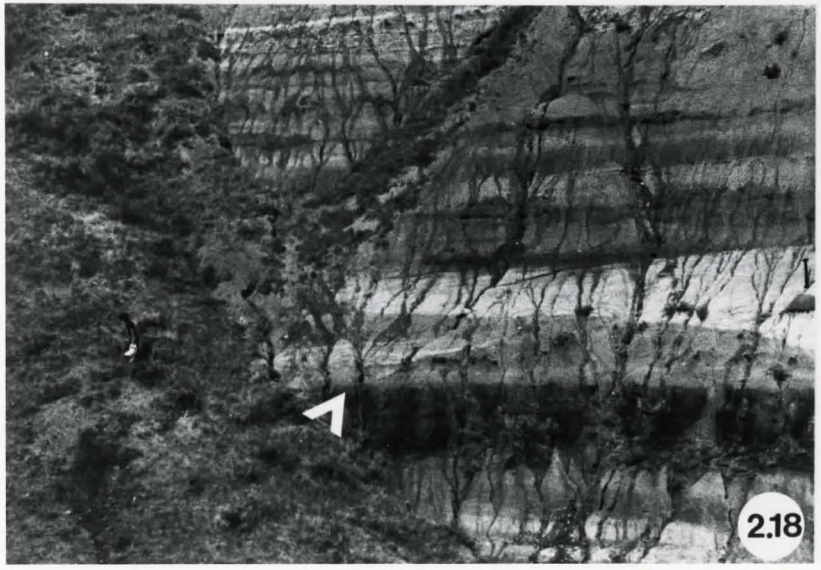
2.18


2.16

The shale contains fine coalified organic matter.

Interpretation:

The grey shale represents the deposition in a quiet environment of organic rich fines. The sand stringers may indicate a sudden influx of small quantities of coarse sediment.

CHAPTER 3

CROSS-SECTIONAL GEOMETRY OF THE CHANNELS

On the following pages are brief descriptions of the main morphological features of each of the channels. Included are cross-sectional diagrams showing the locations of the various facies as well as detailed stratigraphic sections corresponding to the cross-sections.

Paleocurrent directions were determined for each channel from three sedimentary structures, trough cross-bed dips, accretion surface strikes and the orientation of rib and furrow structures. Paleocurrent roses, with the calculated mean flow direction are included with the channel cross-sections.

Channel 1:

Channel 1 is a sand filled channel with an apparent width of 43.6 m and a maximum sand thickness of 4.7 m. The section visible in outcrop is slightly oblique to the channel cross-section. The main characteristics of this sand body are a concave upward base, a flat top, and large, concave-upward channel-fill strata. The concave-upward surfaces are emphasized by the concentration of "coffee grounds" on the bedding surfaces. The "coffee grounds" are

LEGEND

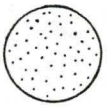

Sandstone

Shale

Coal

Carbonaceous Shale

Lateral Accretion Surface

Trough X-bedding

Mudclast

Tabular Mudclast

Coal Clast

"Coffee Grounds"

Ripple X-lamination

Convolute Lamination

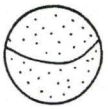

Concave Upward Surface

Paleoflow Directions:

i) Trough Limbs-Dip dir.

ii) Lateral Accretion Surfaces-Dip dir.

iii) Rib and Furrow

extremely abundant in the lower half of the sand body and are less abundant in the upper half.

The channel truncates the laterally adjacent grey shale (Facies 8) and point bar (Facies 5) to the north. To the south are the interfingering shales and sands of facies 4.

The channel sand is topped by a thin layer of carbonaceous shale (Facies 7).

Paleoflow Direction:

Paleoflow measurements derived from the dips of trough limbs give a mean flow direction to the ESE. The rib and furrow structures show a flow direction of 66 degrees. The paleoflow measurements obtained from the rib and furrow structures are slightly oblique to the lateral accretion surfaces mean strike of 81 degrees.

Figure 3.1 Channel 1. Scale is 1 m.

CHANNEL 1

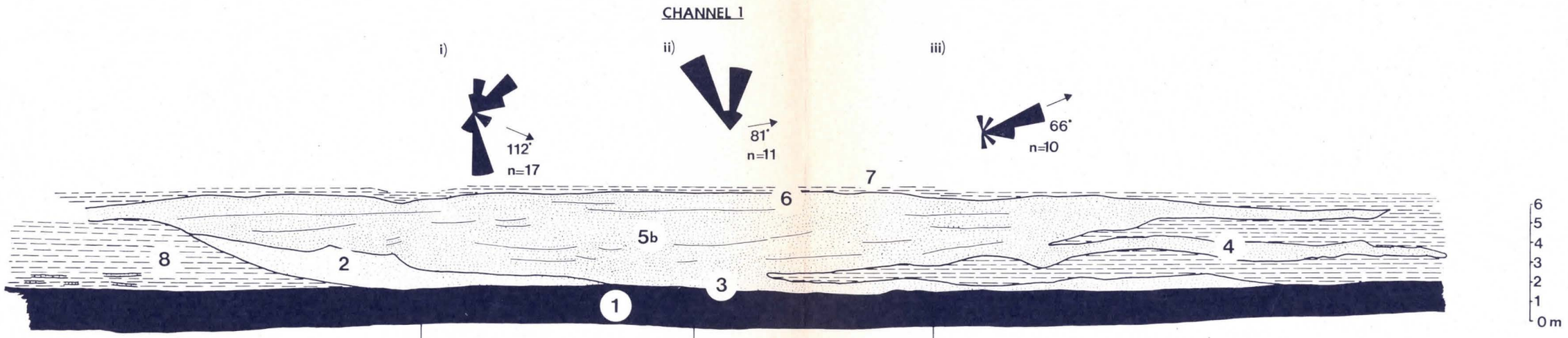
i)
112°
n=17
ii)
81°
n=11
iii)
66°
n=10
7
6
5b
4
8
2
3
1
6
5
4
3
2
1
0 m

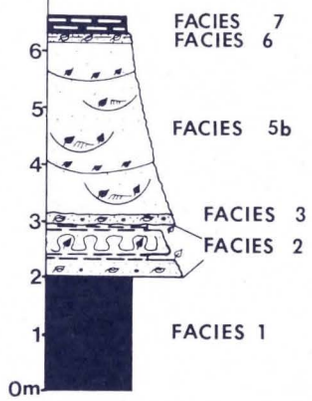
FACIES 7
FACIES 6
FACIES 5b
FACIES 3
FACIES 2
FACIES 1
6
5
4
3
2
1
0m

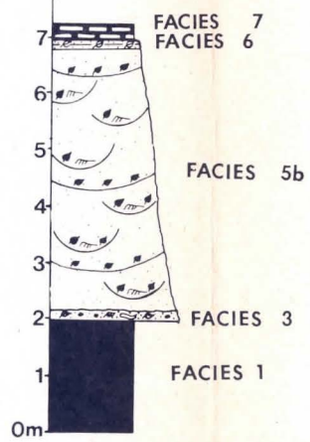
FACIES 7
FACIES 6
FACIES 5b
FACIES 3
FACIES 1
7
6
5
4
3
2
1
0m

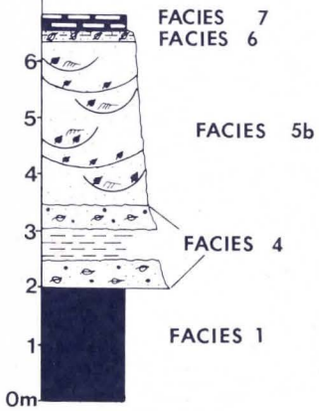
FACIES 7
FACIES 6
FACIES 5b
FACIES 4
FACIES 1
6
5
4
3
2
1
0m

Channel 2:

The sand body which comprises Channel 2 is more extensive and tabular shaped than the sand body of Channel 1. Due to the incomplete nature of the outcrop, only a minimum sand body width of 84 m can be obtained. The maximum sand body thickness is 4 m.

The north edge of the channel is not well defined due to the fact that the sand appears to grade into shale. An elongate sand body occurs above the north edge of the channel where the sand grades into the shale. It appears to dip towards the north.

The north half of the channel cross-section contains well defined, low angle dipping surfaces that dip in the south-east direction.

The south edge of the channel contains large scale trough cross-bedding. Lateral accretion surfaces are not present in the southern portion of the channel.

The carbonaceous shale, which caps each of the channels is present below Channel 2 and has a gradational contact with the coal. Its contact with Channel 2 is erosional.

Paleoflow Directions:

The paleoflow directions determined from Channel 2 are consistent with the values obtained from Channel 1, showing a dominantly eastward trend.

The paleocurrent measurements taken from the dip direction of trough limbs give ESE directions whereas rib and furrow orientations indicate flow directions towards the

ENE. Lateral accretion surfaces strike almost parallel to flow directions obtained from the rib and furrow structures.

Figure 3.2 Channel 2. Scale is 1 m.

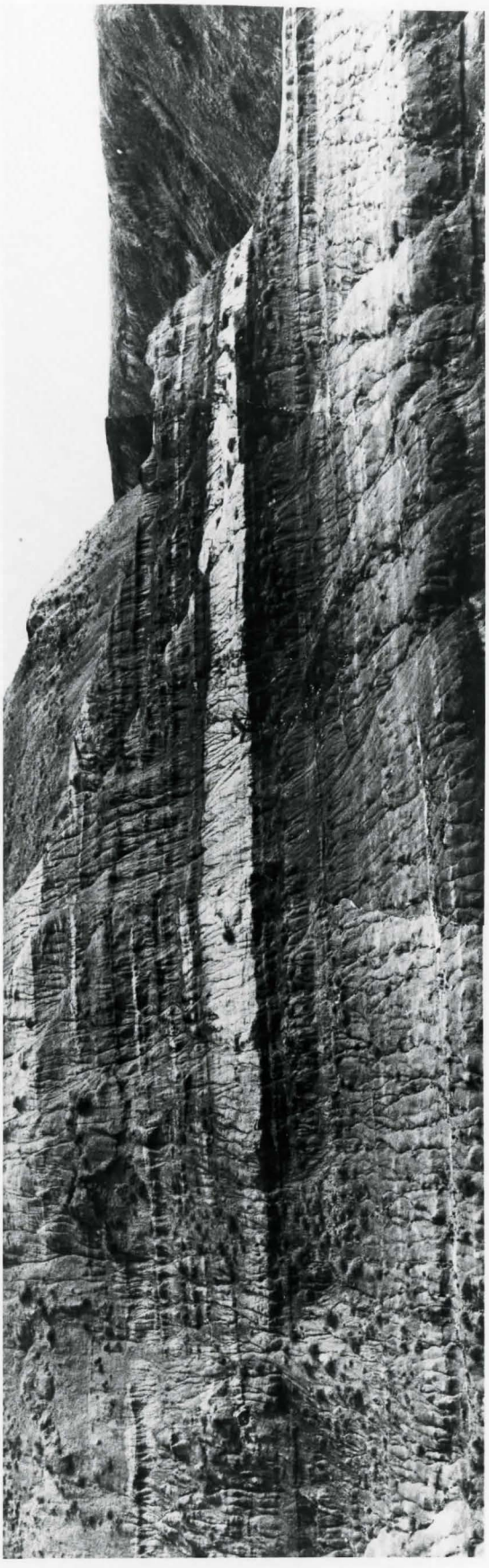

CHANNEL 2

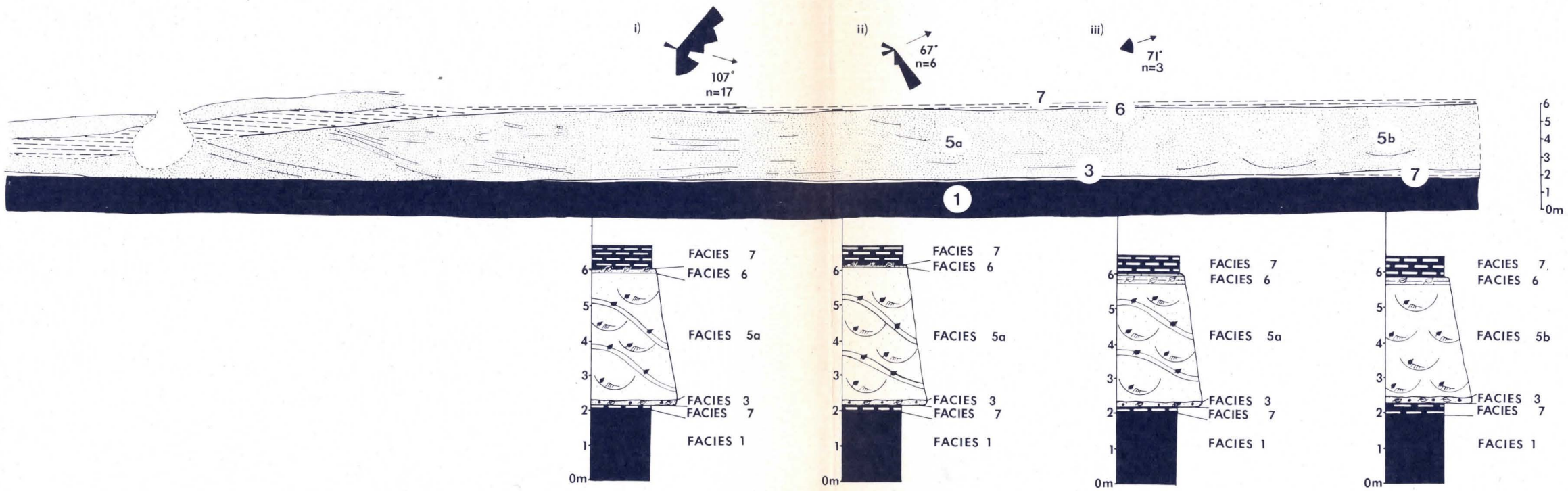
i)
107°
n=17
ii)
67°
n=6
iii)
71°
n=3
7
6
5a
5b
3
7
1
6
5
4
3
2
1
0m
FACIES 7
FACIES 6
FACIES 5a
FACIES 3
FACIES 7
FACIES 1
FACIES 7
FACIES 6
FACIES 5a
FACIES 3
FACIES 7
FACIES 1
FACIES 7
FACIES 6
FACIES 5a
FACIES 3
FACIES 7
FACIES 1
FACIES 7
FACIES 6
FACIES 5b
FACIES 3
FACIES 7
FACIES 1

Channel 3:

Channel 3 is similar in its general shape to Channel 1. The sand body is lenticular with a width of 49 m and a maximum thickness of 4.5 m.

The internal features of this channel sand are markedly different from those of Channel 1. The sand contains well defined lateral accretion surfaces. Obvious scour surfaces are also a notable feature of this sand. Lateral accretion surfaces are truncated by the scouring surfaces and are overlain by sands containing lateral accretion surfaces with a different orientation. At least 4 episodes of scouring are evident (see fig. 3.7).

A thick layer of carbonaceous shale occurs above the sand at the north end of the channel. The carbonaceous shale is also present filling concave upward scours present at the top of the point bar sand.

Paleocurrent Directions:

The dips of the trough limbs give a northeast paleoflow direction whereas ENE and east directions were obtained from the orientation of lateral accretion surfaces and ripple cross lamination. The ripples are oriented obliquely to the lateral accretion strikes.

Due to the rarity of hoodoos, where ripple structures are preserved, only one orientation from ripple cross lamination was obtained.

Figure 3.3 Channel 3. Scale is 1 m.

CHANNEL 3

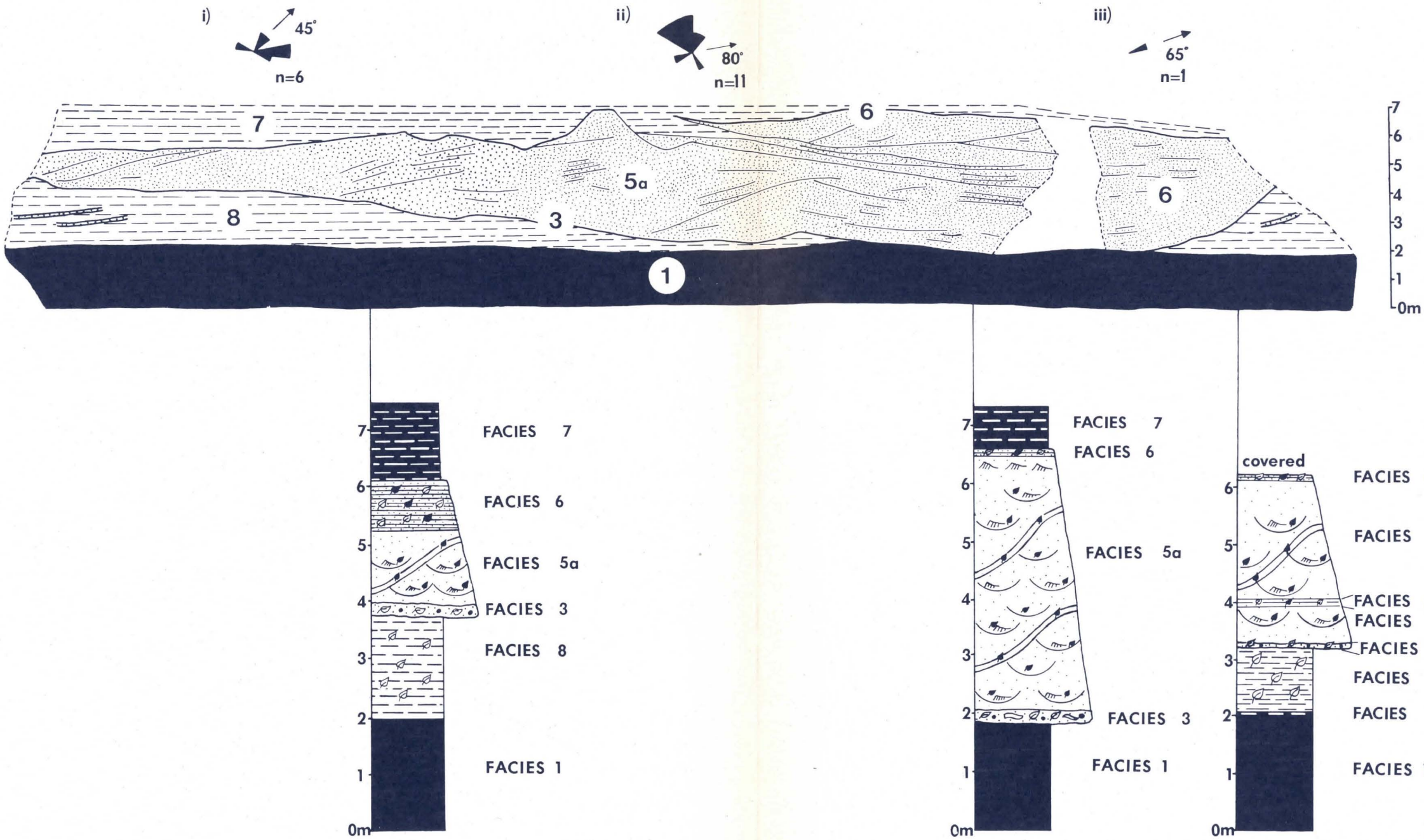
i)
45°
n=6
ii)
80°
n=11
iii)
65°
n=1
7
6
5a
8
3
1
6
7
6
5
4
3
2
1
0m
FACIES 7
FACIES 6
FACIES 5a
FACIES 3
FACIES 8
FACIES 1
FACIES 7
FACIES 6
FACIES 5a
FACIES 3
FACIES 1
covered
FACIES 6
FACIES 5a
FACIES 6
FACIES 5a
FACIES 3
FACIES 8
FACIES 7
FACIES 1

Figure 3.4 Scouring events in Channel 3.

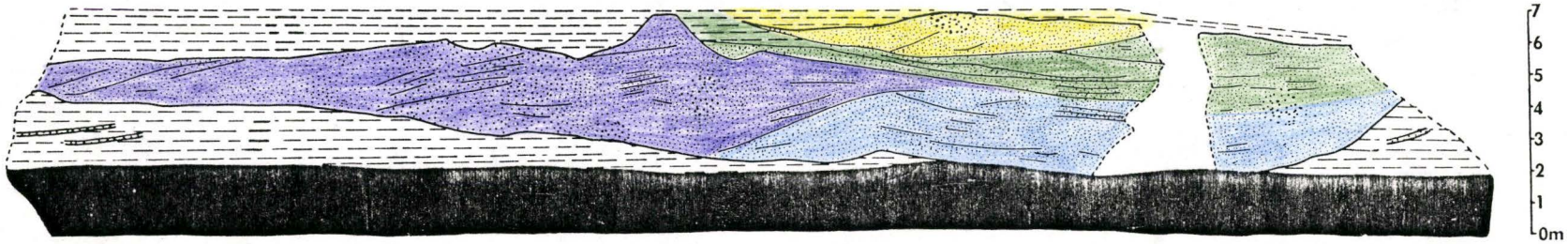

Scouring Events

1 2

3 4

CHAPTER 4

GRAIN SIZE ANALYSIS

Grain size distributions are useful in the interpretation of the hydraulic conditions under which a sediment sample was deposited. When plotted on logarithmic probability paper, the size distribution of a sediment sample commonly exhibits straight line segments separated by discontinuities or "breaks". The line segments have been suggested to represent populations of sediment sorted by different transport mechanisms, with the breaks occurring at the grain size boundaries between these subpopulations (Middleton, 1976).

The three mechanisms by which sediments are transported through a fluvial system are traction, in which grains move by rolling or sliding along the bed, intermittent suspension, where the grains are transported in suspension but return frequently back to the bed, and continuous suspension. Material moved near the bed through traction is referred to as bed load, and material suspended in the main flow, even for only a short period of time is called suspended load. Most of the bed material actually moves in intermittent suspension since most sand moves under high

discharge conditions (Middleton, 1976). Bed material may move in suspension for relatively long distances and may move as bed load for a short distance immediately prior to deposition. Continuously suspended fines are referred to as wash load.

The hydraulic regime of the channel directly affects the concentrations and rate of movement of bed load and intermittently suspended material. The abundance and rate of movement of the fine material transported as wash load do not depend directly on the hydraulics of the flow. Because rivers have an almost unlimited capacity for transporting fines, the concentration of washload is mainly dependant on the rate of supply.

The shear stress on the bed determines the largest grain size that can be moved by traction and the largest particle that can be moved by intermittent suspension. The the breakpoint between the bedload and intermittently suspended population represents the maximum grain size that can be carried in suspension. From this, the bed shear stress and shear velocity can be determined using a critical ratio between the settling velocity of the grain and the shear velocity. In order for suspension to occur, the settling velocity of the grain must be less than or equal to the shear velocity of the flow (Middleton, 1976). The breakpoint represents the grain size at which the settling velocity and shear velocity are equal.

In order to make hydrologic interpretations from grain size distributions, the following assumptions must be made; i) the grain size distribution is a result of hydraulic sorting, ii) the grain size distribution shows no reflection on the source (except in the case of the percentage of washload), and iii) little grain breakage occurred during sieving.

Methods:

To determine the grain size distribution and to estimate shear velocities for the channels, sand samples from each sand facies in Channel 1 and samples from Facies 5 of channels 2 and 3 were disaggregated and grain sizes were separated by dry sieving (for sieving methods, see Appendix A, for sample locations see fig. 4.1).

Cumulative frequency versus grain size (phi units) were plotted for each sample on logarithmic probability paper. The resultant graphs are contained in figures 4.3 through 4.8.

Results and Discussion:

Two distinct types of grain size distribution plots are shown by figures 4.3 through 4.8. These distributions will be referred to as Type 1 and Type 2 (fig. 4.2) and will be used to describe the samples. The Type 1 distribution is comprised of three line segments; a tail of coarse, generally poorly sorted material that is transported by traction, a well sorted population of intermediate grain sizes that are carried in intermittent suspension, and a

tail of poorly sorted washload. The Type 2 distribution lacks the coarse tail component of the Type 1 distribution and consists only of the intermittently and contiuously suspended populations.

The grain size distributionswill be discussed according to the facies from which the samples were taken.

FACIES 2 (fig. 4.3)

Samples 31 and 32 resemble the Type 2 distribution due to the absence of a coarse tail, indicating that all the sediment was transported as suspended or as intermittently suspended material. The only major difference between the samples is the greater proportion of washload in sample 32 as compared to sample 31. In both samples, the breakpoint between the two populations is .09 mm.

FACIES 4 (fig. 4.4)

Sample 11, representing the sand of facies 4, shows a Type 2 distribution with the breakpoint occuring at a grain size of .09 mm

FACIES 5b (figs. 4.5 and 4.6)

The samples from facies 5b in Channel 1, with the exception of sample 25, can be described as a Type 2 grain size distribution pattern.

The curves for samples 24, 26 and 28 are similar although samples 24 and 26 show a slight kink in the coarse end of the curve. The breakpoint between intermittently and continuously suspended load occurs at a value of .12 mm for all three samples.

Sample 25 shows a distinct Type 1 distribution which is evident by the pronounced coarse tail. The breakpoints for this sample correspond to grain sizes of .29 mm and .15mm.

FACIES 6 (fig. 4.7):

Sample 29, which represents the finely laminted sand, lacks a coarse tail and is therefore classified as a Type 2 distribution. The breakpoint of .11 mm is similar to values obtained for samples 24 and 26, thus may have been deposited under similar hydraulic conditions. The presence of the kink in the coarse end of the curve may be anomalous.

FACIES 5a (fig. 4.8):

The grain size distribution for sample 65, from Channel 2, is a Type 2 distribution but appears to contain a large proportion of coarse sediment. On examination of the coarse fractions it was found that at sizes up to 2 0, many of the grains were actually grain aggregates held together by siderite cement that were not fully disaggregated. This resulted in anomalously high values for the proportions of the coarse fractions and low estimates for the finer grain sizes.

Sample 70 from Channel 3 shows a typical Type 2 distribution. The breakpoint between populations is represented by a grain size of .12 mm.

Figure 4.1 Sample locations in Channel 1.

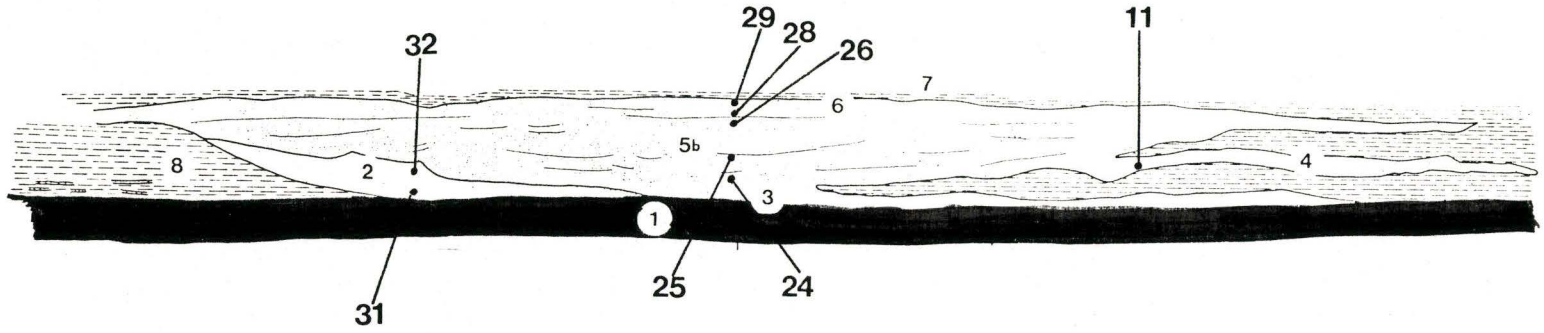
29
28
26
11
32
7
6
5b
8
2
4
3
1
31
25
24

Figure 4.2 Grain size distribution plot types. Line segment 1 represents material transported by traction, line segment 2 represents the population transported in intermittent suspension and segment 3 represents washload material.

GRAIN SIZE DISTRIBUTION PLOTS

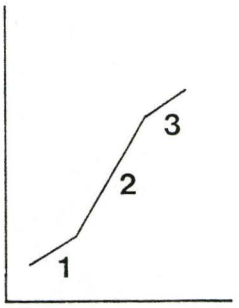

TYPE 1

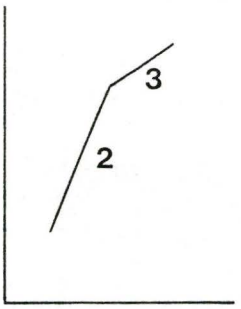

TYPE 2

Figure 4.3 Samples 31 and 32 from Facies 2.

Figure 4.4 Sample 11 from Facies 4.

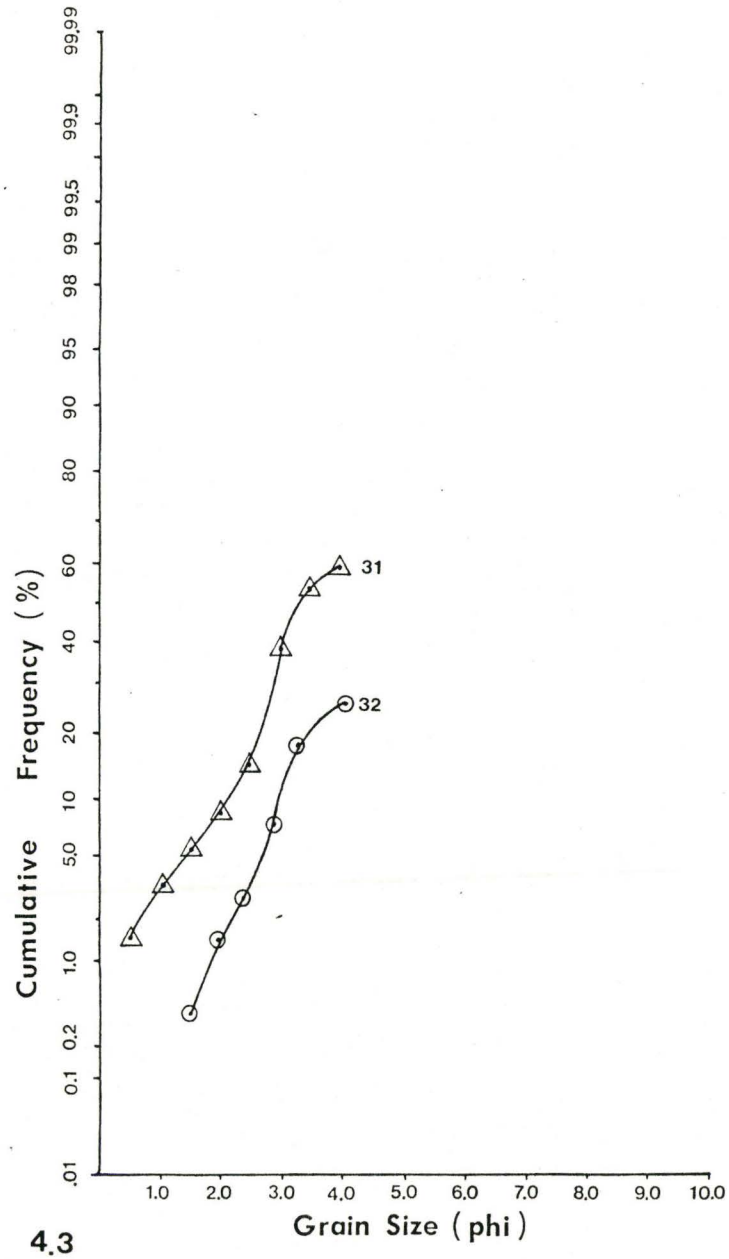
Cumulative Frequency (%)
99.99
99.9
99.5
99
98
95
90
80
60
40
20
10
5.0
1.0
0.2
0.1
.01
1.0
2.0
3.0
4.0
5.0
6.0
7.0
8.0
9.0
10.0
Grain Size (phi)
31
32

4.3

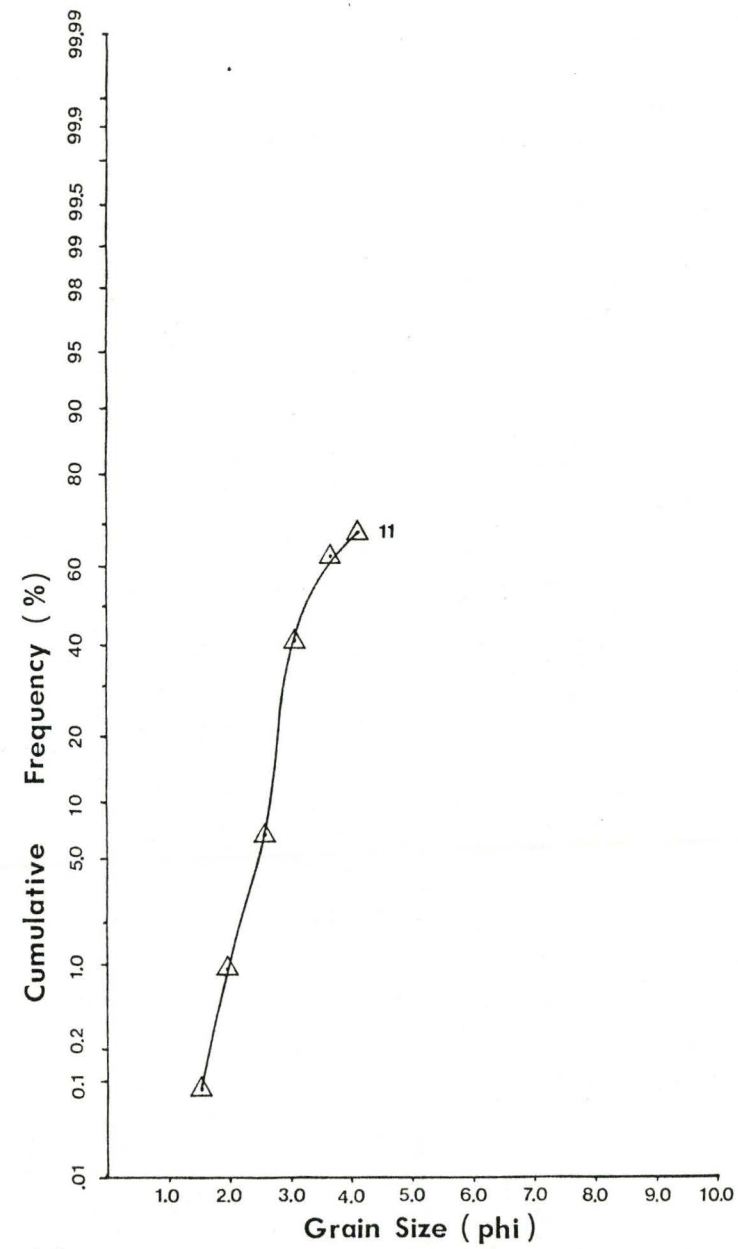
Cumulative Frequency (%)
99.99
99.9
99.5
99
98
95
90
80
60
40
20
10
5.0
1.0
0.2
0.1
.01
1.0
2.0
3.0
4.0
5.0
6.0
7.0
8.0
9.0
10.0
Grain Size (phi)
11

4.4

Figure 4.5 Samples 24 and 25 from Facies 5b, Channel 1.

Figure 4.6 Samples 26 and 28 from Facies 5b, Channel 1.

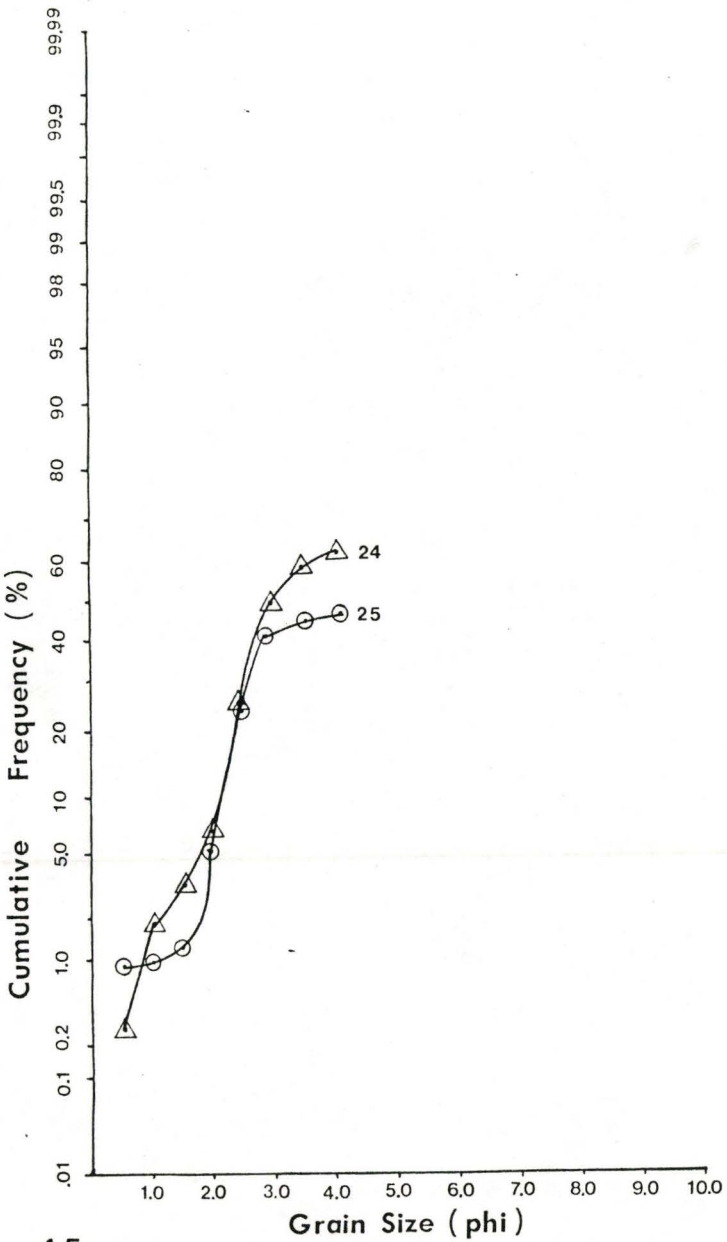
Cumulative Frequency (%)
.01
0.1
0.2
1.0
5.0
10
20
40
60
80
90
95
98
99
99.5
99.9
99.99
1.0
2.0
3.0
4.0
5.0
6.0
7.0
8.0
9.0
10.0
Grain Size (phi)
24
25

4.5

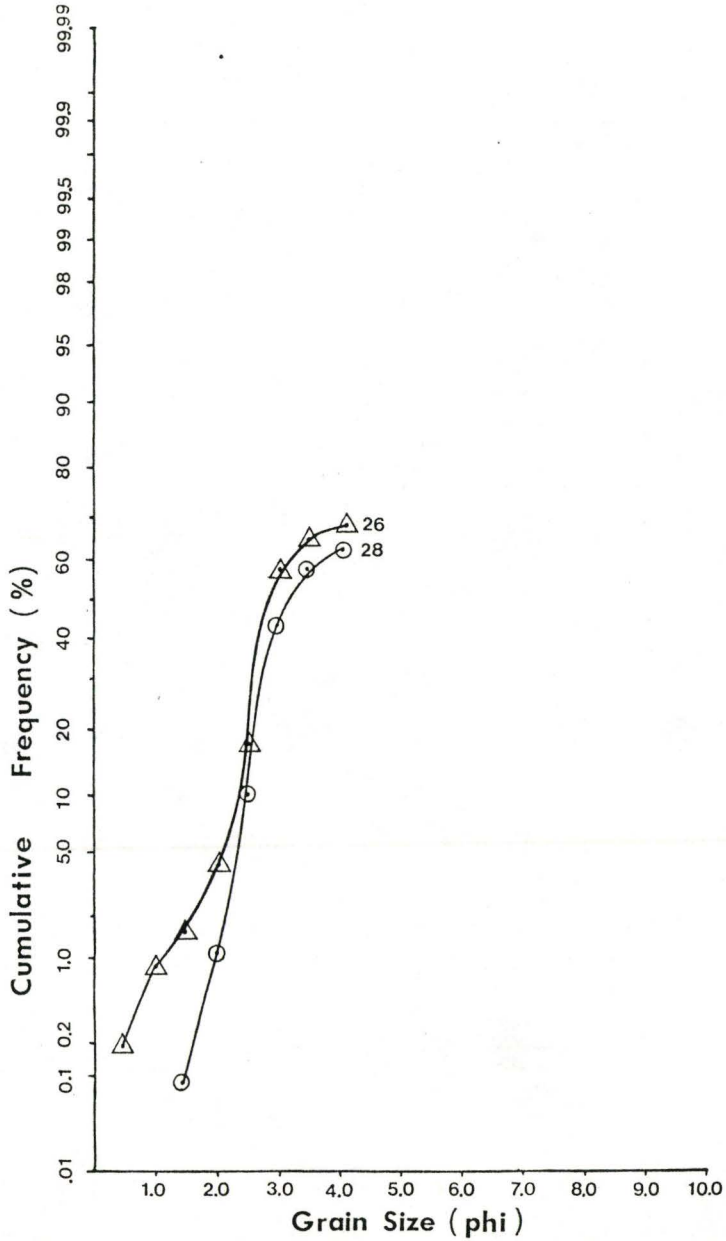
Cumulative Frequency (%)
.01
0.1
0.2
1.0
5.0
10
20
40
60
80
90
95
98
99
99.5
99.9
99.99
1.0
2.0
3.0
4.0
5.0
6.0
7.0
8.0
9.0
10.0
Grain Size (phi)
26
28

4.6

Figure 4.7 Sample 29 from Facies 6, Channel 1.

Figure 4.8 Samples 64 from Channel 2 and 70 from Channel 3.

4.7

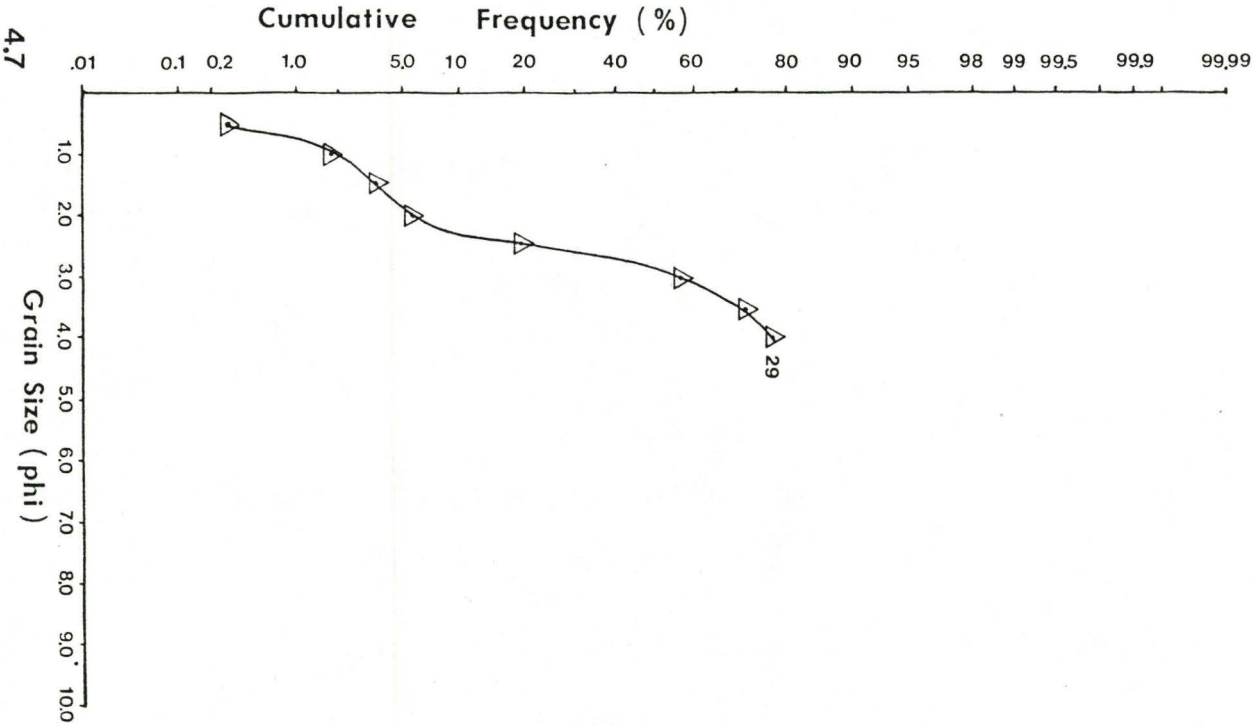
Cumulative Frequency (%)
.01 0.1 0.2 1.0 5.0 10 20 40 60 80 90 95 98 99 99.5 99.9 99.99
Grain Size (phi)
1.0 2.0 3.0 4.0 5.0 6.0 7.0 8.0 9.0 10.0
29

4.8

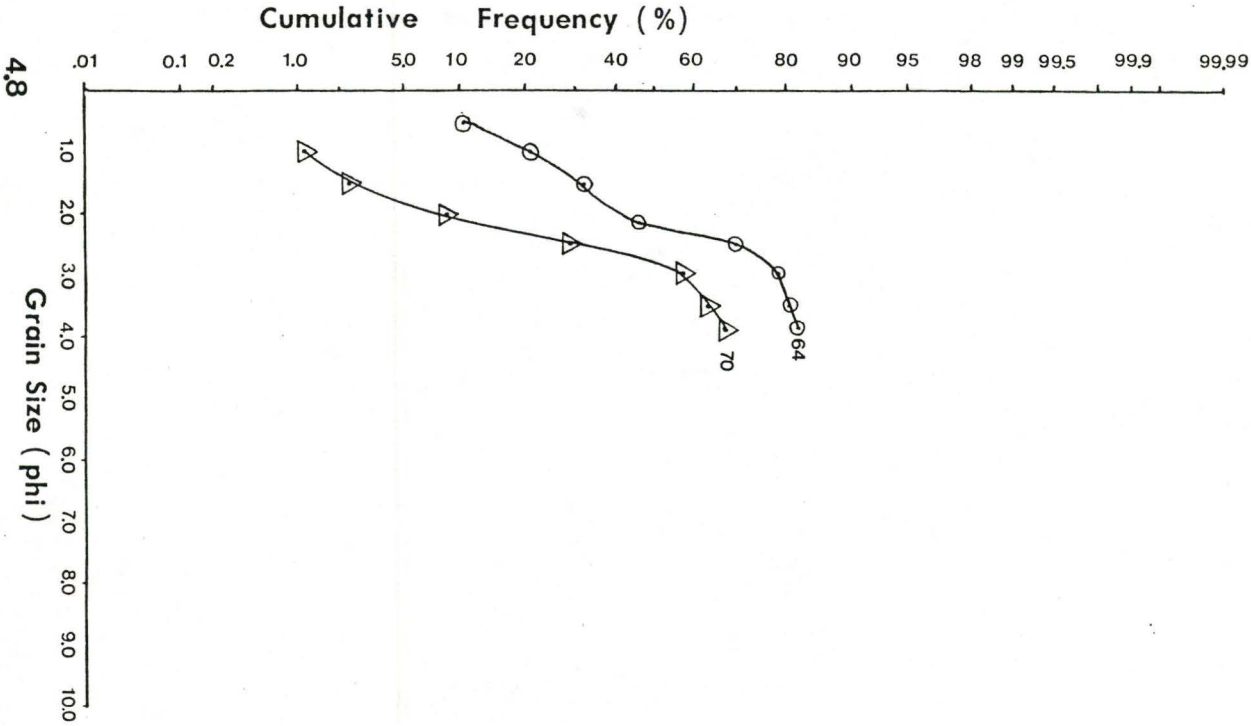
Cumulative Frequency (%)
.01 0.1 0.2 1.0 5.0 10 20 40 60 80 90 95 98 99 99.5 99.9 99.99
Grain Size (phi)
1.0 2.0 3.0 4.0 5.0 6.0 7.0 8.0 9.0 10.0
64
70

Discussion of Grain Size Distribution Plots:

From the grain size graphs, four common features were noted: i) the poorly sorted nature of the bedload (when present) as compared to the intermittently suspended load, ii) the relatively large proportion of intermittently suspended material, iii) the large population of poorly sorted washload and iv) the lack of a coarse tail in many samples.

The traction population is probably less well sorted than the intermittently suspended population because in the presence of ripples or dunes, the rate of movement of the grains in traction is determined by the rate of migration of the bedforms. Thus grain size will have little effect on the movement of the bedload as long as the flow is competent to move the largest grains present (Middleton, 1977).

The intermittently suspended population is prominent in the samples because major deposits of sand tend to form in environments where sand can be taken into suspension, but is deposited before it can be rapidly removed from the environment. The well-sorted nature of this population is a result of repeated suspension and deposition which is an efficient hydraulic sorting mechanism.

The abundance of the suspended population is more strongly dependant on the source than on hydraulic sorting, thus a large amount of fine material was supplied to the channels. Determination of the depositional size distribution is difficult because the fine sediment may have

been modified through flocculation or organic binding before deposition.

The lack of a coarse tail may indicate that either the flow was not competent to to move large grains or, more probably, there was no supply of coarse material to comprise the coarse tail. In the following section, the competence of the flow will be calculated.

FLOW CALCULATIONS:

Grain size distribution graphs yield information that can be used in determining the characteristics of the flow in which the grains were transported.

Sediments of a given grain size will not move by traction until a certain shear velocity (U^*) is reached. The suspension of grains occurs when the shear velocity is greater than or equal to the settling velocity of the grains.

The breakpoint between the material moved as traction and intermittently suspended material in a Type 1 grain size distribution represents the grain size at which the shear velocity (U^*) is equal to the settling velocity of the grain (W). From figure 4.9 (Blatt et al., 1980) which illustrates the curve for grain suspension, the shear velocity of the flow can be determined for the breakpoint grain size.

Figure 4.9 Criteria for the initial movement and suspension of quartz grains in water at 20 C.(Blatt et al., 1980).

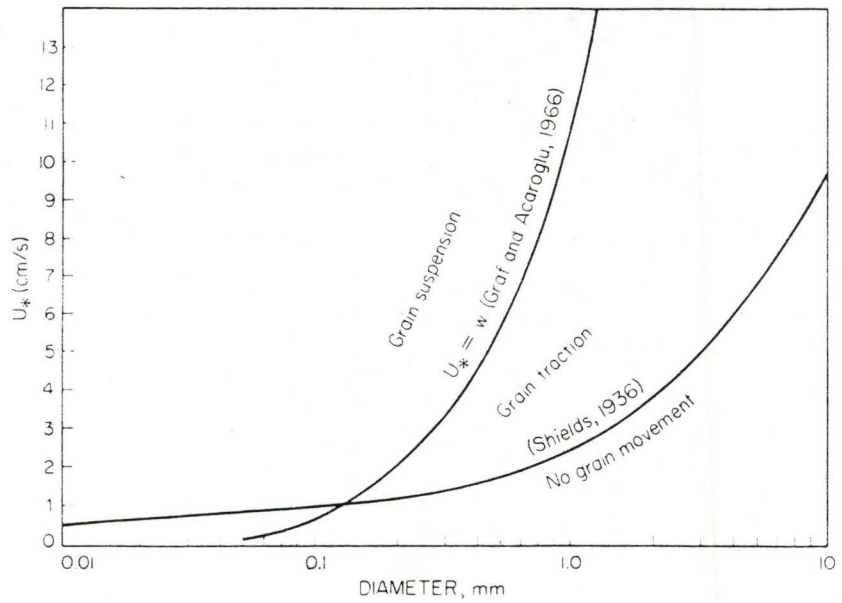
13
12
11
10
9
8
7
6
5
4
3
2
1
0
U* (cm/s)
0.01
0.1
1.0
10
DIAMETER, mm
Grain suspension
U* = w (Graf and Acaroglu, 1966)
Grain traction
(Shields, 1936)
No grain movement

The shear velocity of the flow (U*) can be related to the average velocity of the flow by the equation:

$$\frac{U}{U^*} = \frac{C}{\sqrt{g}}$$

where $C/\sqrt{g}$, the dimensionless Chezy coefficient, is dependant on the roughness of the bed. Values for the Chezy coefficient, where dunes are the dominant bedforms, range from 7.0 to 13.2. In the case of plane beds, the Chezy coefficient ranges from 16.3 to 20.0 (Graf, 1971).

The shear stress on the bed (τ_o) is related to U^* by the equation:

$$U^* = \sqrt{\tau_o/\rho}$$

In the case of water where $\rho = 1$, $\tau_o = U^{*2}$

The majority of the grain size plots in this study represent Type 2 distributions, thus lack a coarse tail. The grain size at which $U^* = W$ cannot be determined but from the coarsest grain size on the plot, a minimum value for U^* can be estimated.

To determine the competence of the flow, or sediment size that it can move on the bed, the following formula can be used;

$$\beta = \frac{\tau_o}{(\gamma_s - \gamma)d}$$

where β = Shield's Beta, which, for turbulent flows (Reynolds number > 1000) is equal to .06. γ_s is the specific weight of the grain, γ is the specific weight of the fluid and d is the diameter of the largest grain that can be moved on the bed. For quartz grains, γ_s is equal to .2597 g cm^{-1} s^{-2}. γ for water is equal to 980 g cm^{-1} s^{-2}.

The values of U^*, U, τ_o and competence are tabulated in Table 4.2.

RESULTS AND DISCUSSION OF FLOW CALCULATIONS:

The results in table 4.2 indicate that mean flow velocities in the channel system studied ranged from 28 to 110 cm s^{-1} depending on the value used for the Chezy coefficient, and shear velocities ranging from 3.1 to 9 cm s^{-1}.

Calculationed values of d demonstrate that in all cases the flow was competent to move grain sizes much larger than the maximum grain size present. In samples where a coarse tail is present, the flow was competent to transport, by traction, grains from 3 to 6 times larger than the largest grain size in the sediment sample. In the samples lacking a coarse tail, the flow was competent to move on the bed, grains that range from 4.6 to 12 times larger than the

Table 4.1 Shear velocities, average velocities, shear stress and competence of flow as calculated for the samples. Note that the shear stresses and shear velocities only represent minimum values for all samples except 25, because they lack coarse tails. The minimum and maximum values given for average velocity correspond to the range in the Chezy coefficient.

TABLE 4.1

FACIES	SAMPLE NUMBER	GRAIN SIZE (mm)	U* (cm/s)	C / $\sqrt{g}$		$\bar{U}$ (cm/s)		τ_o (cm^2/s^2)	Ds (mm)
				min	max	min	max		
2	31	0.70	9.0	7.0	13.2	63.0	118.0	81.0	8.3
	32	0.35	4.0	7.0	13.2	28.0	52.8	16.0	1.6
4	11	0.35	4.0	7.0	13.2	28.0	52.8	16.0	1.6
5b	24	0.70	9.0	7.0	13.2	63.0	118.8	81.0	8.3
	25	0.29	3.1	7.0	13.2	21.7	40.9	9.6	0.9
	26	0.70	9.0	7.0	13.2	63.0	118.8	81.0	8.3
	28	0.35	4.0	7.0	13.2	28.0	52.8	16.0	1.6
6	29	0.50	5.5	6.3	20.0	89.7	110.0	30.3	3.1
5a - Channel 2	6	0.70	9.0	7.0	13.2	63.0	118.8	81.0	8.3
5a - Channel 3	70	0.50	5.5	7.0	13.2	38.5	72.6	30.3	3.1

grains present in the sample. It must be noted that although the largest sieve mesh size used was .5 ϕ (.70 mm), it was evident by visual inspection that no grains approached the calculated values for competence of the flow. For several samples, no grains greater than 1.5 ϕ (.35 mm) were present.

The distribution of grains that move by traction may be affected by three limiting conditions: i) availability of material, ii) competence of the flow and iii) the boundary conditions between traction and intermittent suspension as the dominant form of transport (Middleton, 1977).

The results of the grain size analysis indicate that availability is the major factor affecting the characteristics of the bed load population, since it was calculated that in every case the flow was competent to move on the bed, grains of a much larger size than were present.

Since grains that move by traction move more slowly than intermittently or continuously suspended sediments, the probability of the grain being temporarily or permanently deposited is much greater, thus reducing the availability of the larger grain sizes transported as bed load.

The minimum size of the traction population is defined by the suspension criterion thus the size distribution of the bedload is dependent on the shear velocity of the flow.

CHAPTER 5

PETROGRAPHY

To determine the composition and possible provenance of the sands, thin sections from samples of each sandstone facies of Channel 1 and from the main channel sand (Facies 5) of Channels 2 and 3, were examined. The rocks were injected with blue epoxy to enhance the visibility of porosity and the thin sections were cut perpendicular to bedding. Observations were made using a transmitting light microscope under plane polarized and cross polarized light. The petrographic compositon was determined for each thin section by estimating the percentage of each constituent in four randomly chosen fields of view and calculating the average (Table 5.1). The slides were reexamined in random sequence several days later and estimated percentages fell within 12% of previous estimates.

Results:

The major components of the sandstones are quartz, plagioclase feldspar, potassium feldspar, rock fragments and minor biotite, muscovite, sillimanite and iron oxides. The minerals are contained in a clay matrix with minor calcite cement. No visible porosity is present in the samples.

The rocks were classified by plotting modal percentages on a percent quartz vs percent feldspar vs percent rock fragments ternary diagram after Folk (1968). The resulting data plotted within the Lithic Arkose and Feldspathic Litharenite classifications (fig. 5.1).

Table 5.1 Estimated modal composition of thin sections (%).

TABLE 5.1 ESTIMATED PETROGRAPHIC COMPOSITION

CONSTITUENT	6	15	16	29	33	42	64	70
QUARTZ	20%	20%	25%	20%	20%	15%	20%	20%
PLAGIOCLASE	15%	10%	15%	10%	5%	15%	5%	12%
ORTHOCLASE	10%	5%	10%	10%	10%	8%	10%	10%
ROCK FRAGMENTS	15%	25%	15%	25%	20%	20%	20%	15%
OPAQUES	2%	3%	1%	--	2%	2%	1%	1%
CARBONATE	7%	3%	10%	--	trace	5%	15%	8%
OTHER	1%	--	1%	2%	2%	--	--	2%
MATRIX	30%	34%	23%	33%	41%	35%	29%	32%
Q	33%	33%	38%	31%	36%	26%	36%	35%
F	4 %	25%	38%	31%	28%	40%	28%	38%
RF	25%	42%	24%	38%	36%	34%	36%	27%

Figure 5.1 Classification of sandstone samples. (After Folk, 1968)

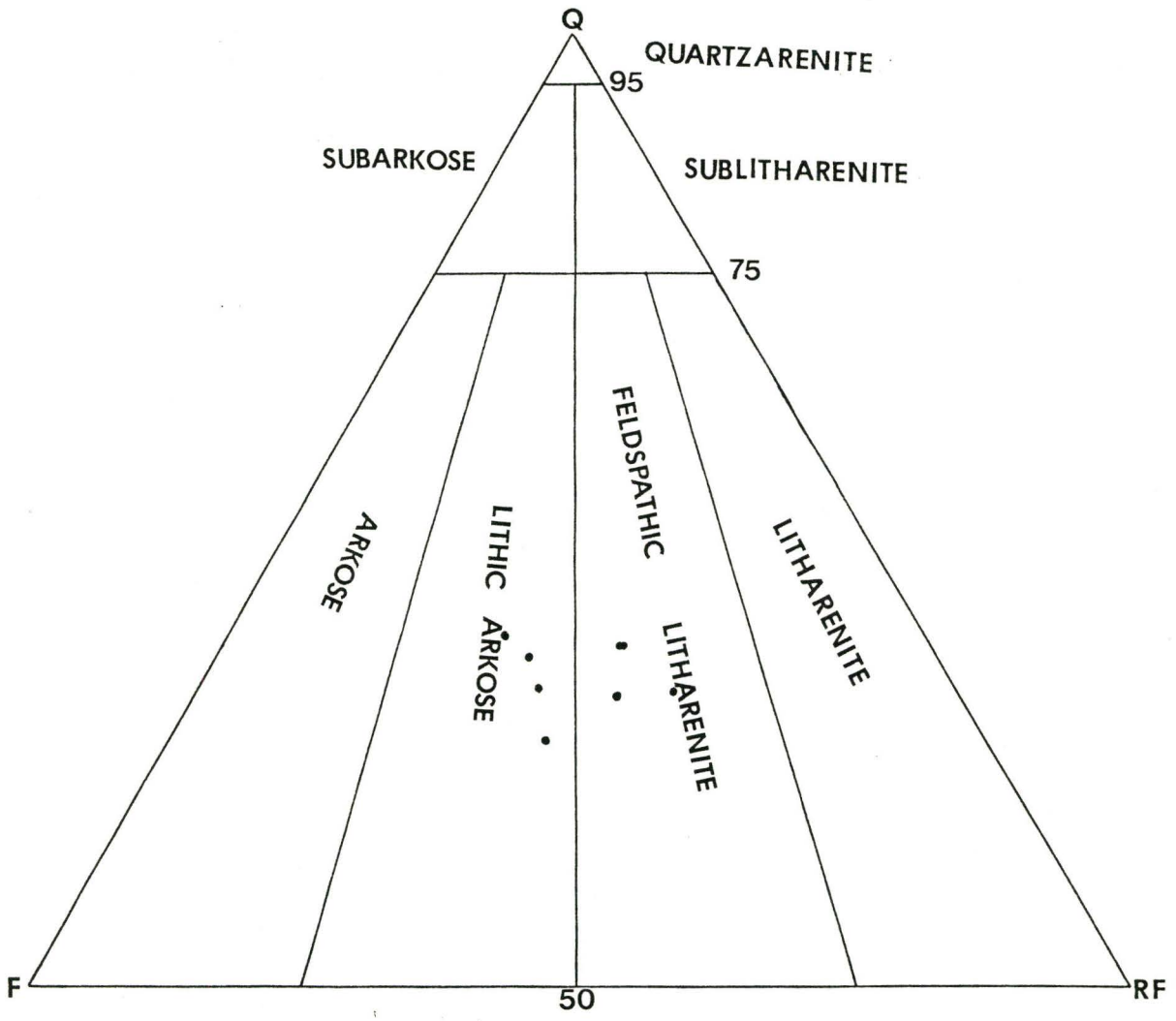
Q
QUARTZARENITE
95
SUBARKOSE
SUBLITHARENITE
75
ARKOSE
LITHIC ARKOSE
FELDSPATHIC LITHARENITE
LITHARENITE
F
50
RF

Quartz:

The quartz present in the thin sections consisted of poorly sorted sub-angular to sub-rounded grains. The grains commonly show dust-like inclusions and often contain inclusions of tourmaline.

The quartz grains were classified into four categories after Basu et al (1975). These are i) monocrystalline grains, ii) polycrystalline with two to three crystals per grain, iii) polycrystalline with more than three crystal per grain and iv) monocrystalline grains that exhibit undulatory extinction. The number of crystal units within a polycrystalline grain has been reported to be related to the source rock. Grains made up of fewer than three crystals are thought to have a plutonic source whereas those grains containing greater than three crystals are believed to have been derived from a metamorphic source.

The provenance of the quartz grains from the channels fall within the low and medium to high rank metamorphic source categories, with most classified as having a low rank metamorphic source (see fig 5.2).

Table 5.2 Abundance of quartz types (%).

TABLE 5.2 TYPES OF QUARTZ

CONSTITUENT	6	15	16	29	33	42	64	70
NON-UNDULATORY	50%	40%	35%	30%	40%	40%	35%	50%
UNDULATORY	50%	60%	5%	70%	60%	60%	65%	50%
POLYCRYSTALLINE (2-3)	15%	10%	15%	10%	10%	15%	10%	20%
POLYCRYSTALLINE (>3)	0%	3%	5%	1%	0%	30%	0%	5%

Figure 5.2 Plot relating types of quartz to provenance of source rocks. (After Basu et al., 1975)

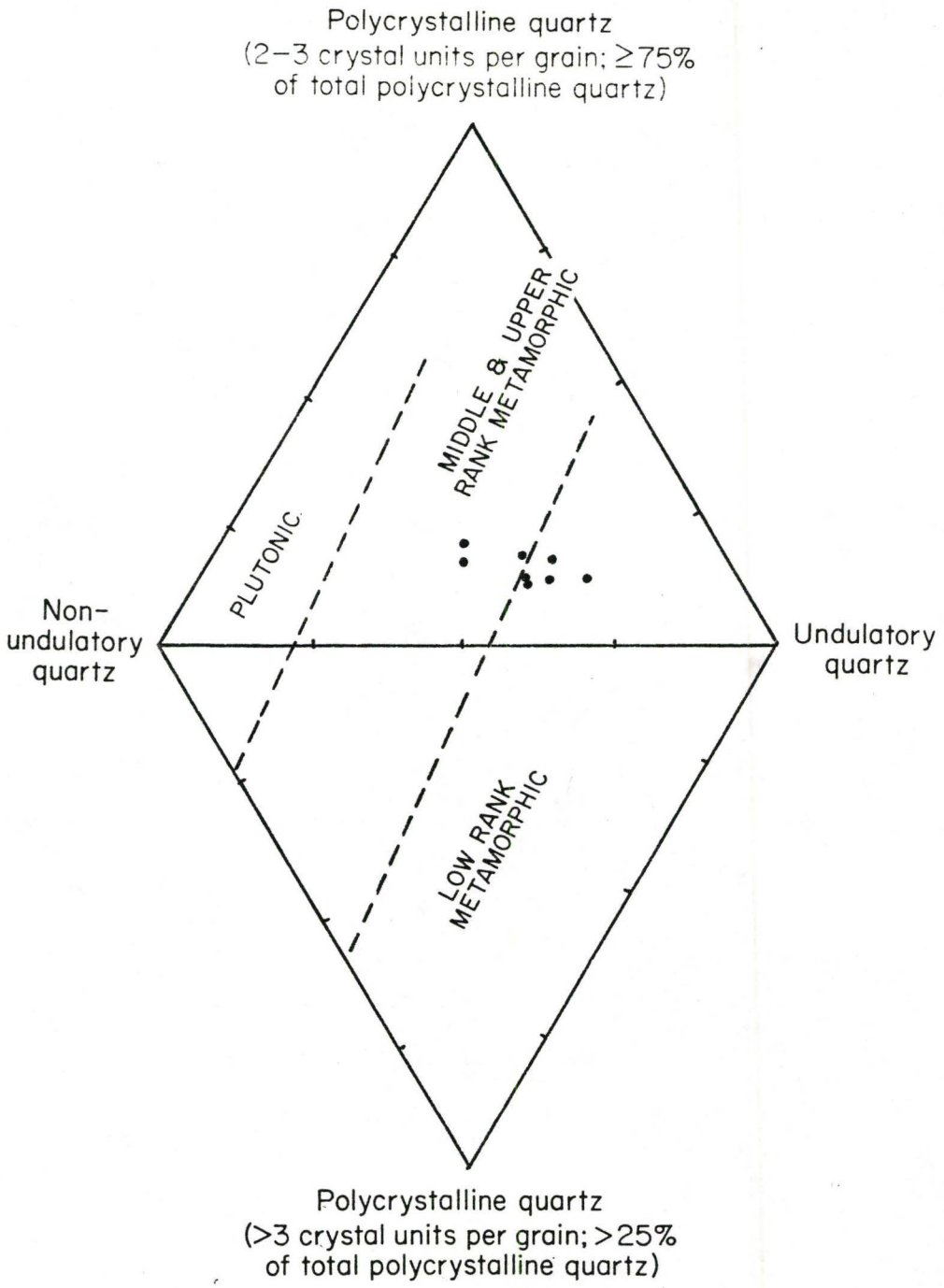
Polycrystalline quartz
(2–3 crystal units per grain; ≥75%
of total polycrystalline quartz)
MIDDLE & UPPER
RANK METAMORPHIC
PLUTONIC
Non-
undulatory
quartz
Undulatory
quartz
LOW RANK
METAMORPHIC
Polycrystalline quartz
(>3 crystal units per grain; >25%
of total polycrystalline quartz)

Plagioclase Feldspars:

The plagioclase feldspars are mainly subangular, and appear to be more angular than the quartz grains. Some of the plagioclase feldspars show evidence of alteration to sericite, although the most common form of alteration of the feldspar is the replacement by calcite. The calcite replacement tends to begin along the grain edges as well as along twin planes and the calcite commonly shows an anhedral morphology.

Replacement of the feldspars by calcite was observed in all thin sections except section 29 (Facies 6) and sample 33 (Facies 2).

Potassium Feldspars:

Carlsbad twinning is common in the potassium feldspars in the thin sections observed. The feldspars are predominantly subangular and in some cases the tabular nature of crystals is partially preserved. The K-feldspars show extensive seriticization.

Rock Fragments:

Three types of rock fagments were observed in the thin sections: chert fragments, volcanic rock fragments and lithic rock fragments. These types were not differentiated during the estimation of modal percentages.

The cryptocrystalline chert occurs predominantly as subrounded to round rock fragments, although some fragments

are distinctly angular. Iron-oxide staining is present on the perimeter of some of the grains.

The volcanic rock fragments are also subrounded to rounded and are composed of fine feldspar laths in a glassy groundmass.

Fine grained mudrock containing quartz and chert comprise the lithic rock fragments. These fragments are well rounded and can be recognized by their brownish colour in plane polarized light.

Rock fragments are abundant in all samples.

Accessory Minerals:

Accessory minerals include muscovite and biotite whcih occur in minor quantites wrapped around the other mineral grains, and an opaque mineral (probably an iron oxide). Tourmaline is present as inclusions in quartz.

Calcite:

As mentioned previously calcite occurs repacing detrital plagioclase grains and as an interstital cement. The amount of calcite in the thin sections does not exceed 15% and is absent in samples 29 and 33.

Matrix:

The consituents of the matrix are difficult to determine due to its fine grained nature but it appears to be composed of clay or mud. It is not known whether the majority of the fine grained material represents detrital or authigenic minerals.

The early cementation by calcite may have reduced the initial porosity to zero, thus preventing the development of authigenic clays in pore spaces.

The shape of the channels tend to favour Schumm's classification of suspended load channels, thus the matrix may consist of mostly detrital material.

Figure 5.3 Sample from Facies 5, Channel 3. Note the subangular quartz grains and well-rounded rock fragments. (Crossed polars, field of view =.4mm)

Figure 5.4 Sample from Facies 5, Channel 1. Note replacement of K-felospar by calcite. (Crossed polars, field of view =.4mm)

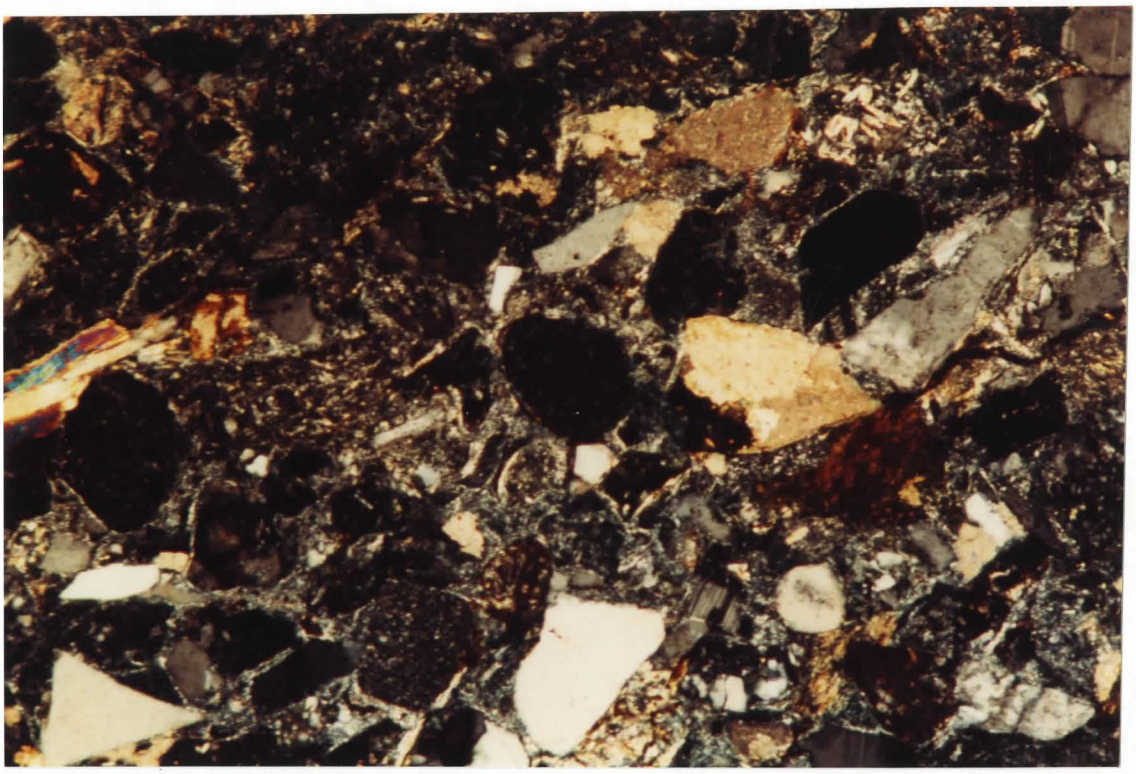

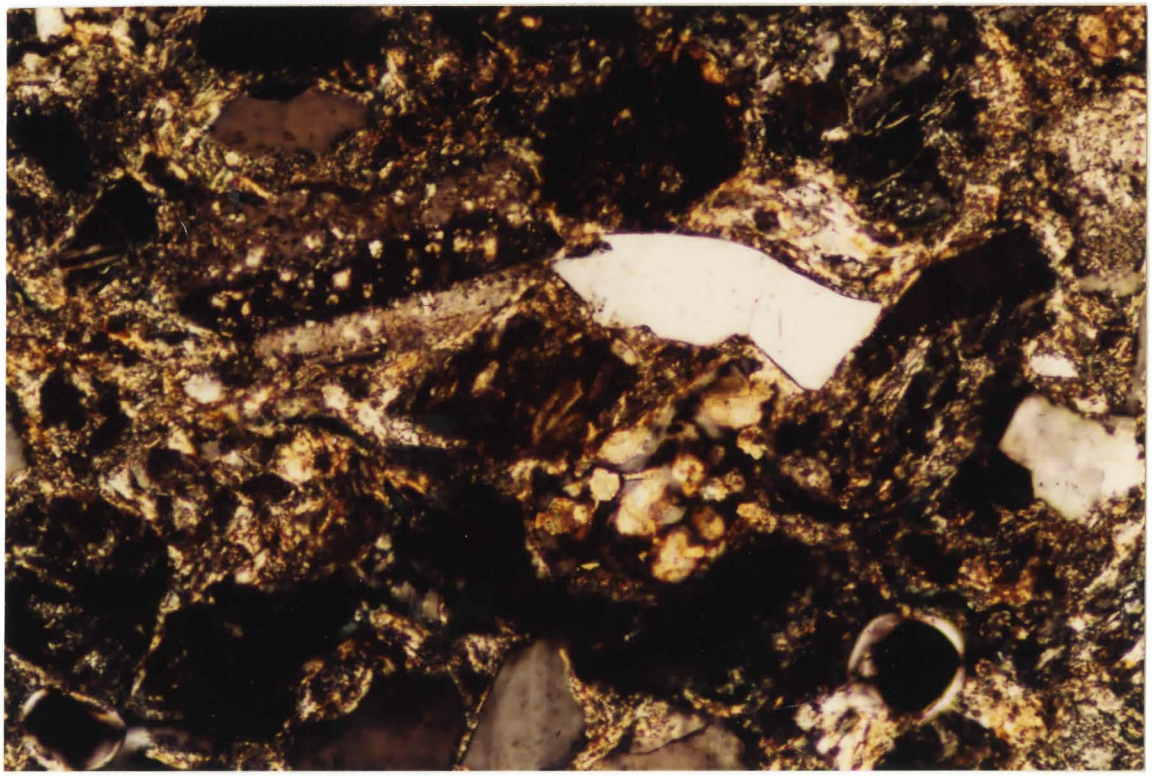

Figure 5.5 Sample from Facies 5, Channel 1. Plagioclase is being replaced by calcite. Note relict albite twinning in the calcite. Crossed polars, field of view = .1mm)

Figure 5.6 Sample from Facies 3, Channel 1. Note well rounded quartz grain. (Double exposure, Crossed polars, field of view=.4mm).

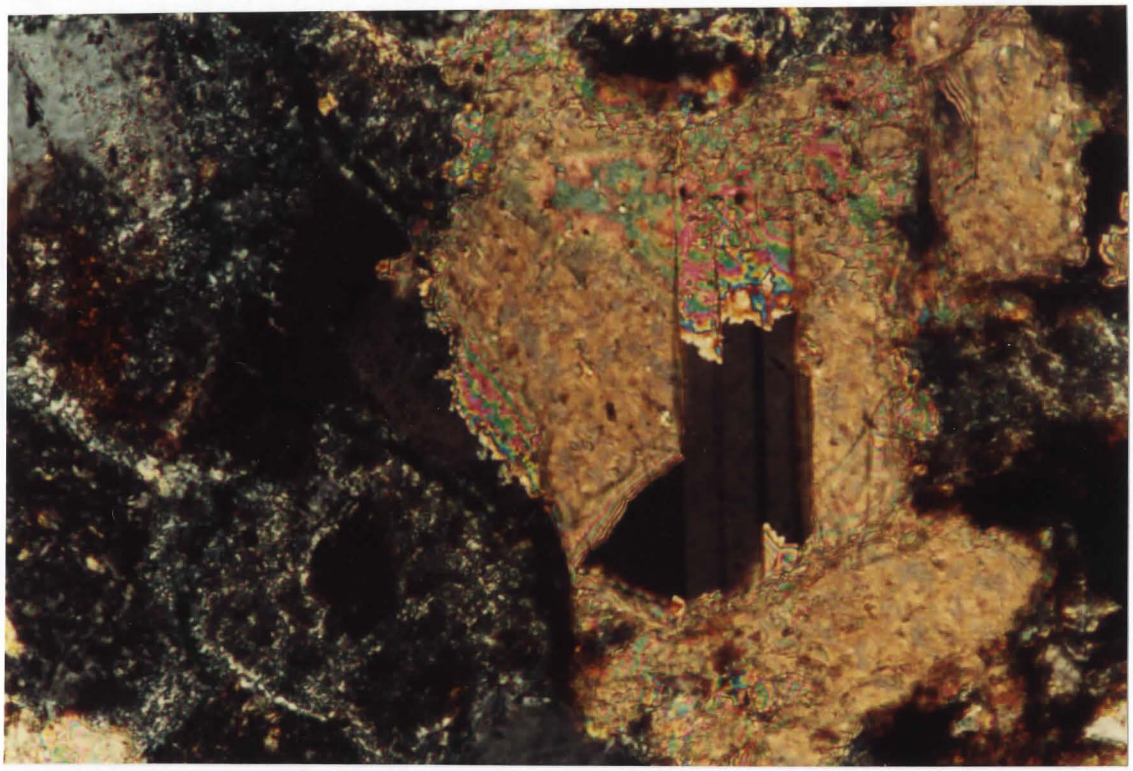

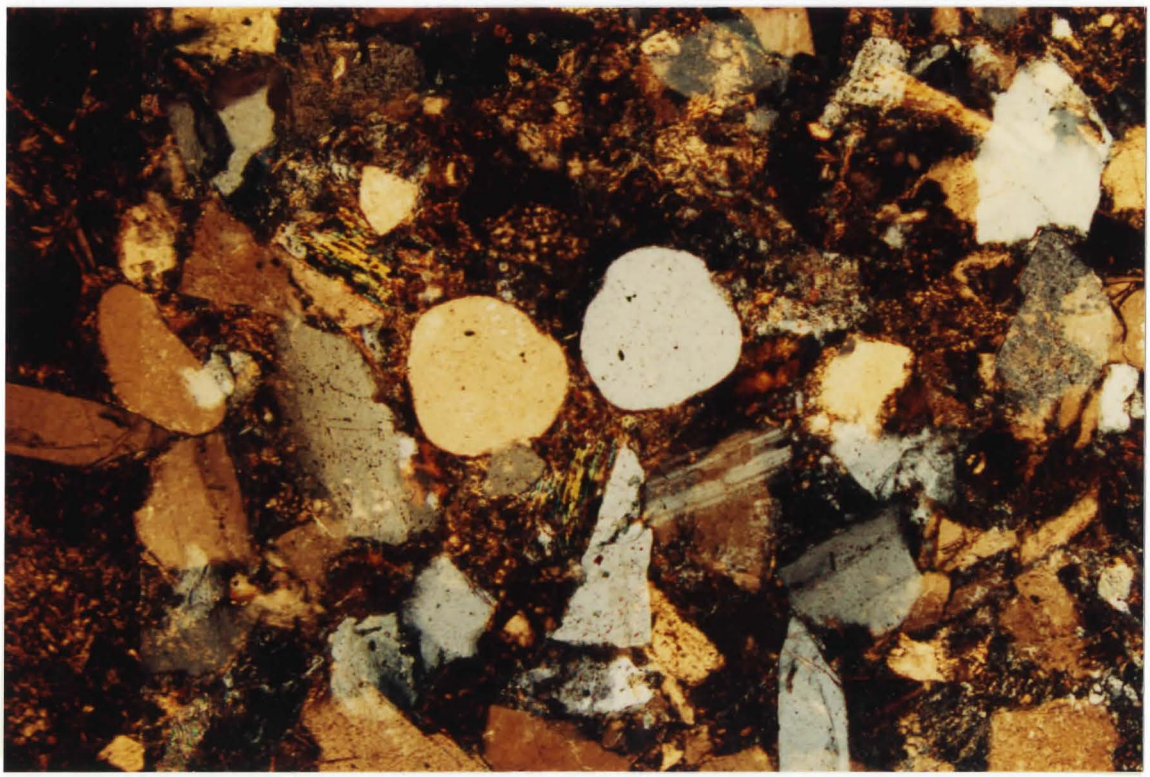

CHAPTER 6

PALEOHYDRAULICS AND PALEOMORPHOLOGY

Empirical relationships between channel morphology and flow characteristics for meandering fluvial systems have been developed by geomorphologists (Leopold and Wolman, 1960, Schumm, 1963,1972) from measurements of modern rivers. These relationships can be applied to the ancient channels in Drumheller to predict flow characteristics and paleomorphology.

The channel parameters required are bankfull stream width (W), bankfull stream depth (D), percent silt-clay in channel bank (Sb) and percent silt-clay in channel bed (Sc). These parmeters are related by regression equations to channel sinuosity (P), meander wavelength (L), meander radius (R), slope (S) and mean annual discharge (Qm).

Two methods of calculating the flow and morphologic characteristics of ancient channels using W, D, Sb and Sc are summarized by Ethridge and Schumm (1978).

The first method involves the use of all four variables. Sc and Sb are used to find the percentage of silt clay in the channel perimeter (M), which reflects the type of load through the channels. Sb and Sc are difficult

to determine in paleochannels because distinctions must be made between detrital and diagenetic clay minerals, which requires thin section petrography and scanning electron microscopy. These difficulties can be overcome by the use of equations developed by Schumm (1972), which relate M to the width-depth ratio, requiring that only W and D be known. Method two of Ethridge and Schumm (1978) is based on this relationship.

Method:

The second method of Ethridge and Schumm (1978) was found to be best suited for the estimation of the morphological and flow characteristics of the channels studied. The excellent and almost continuous exposures and the presence of several well defined lateral accretion surfaces in Channels 2 and 3 facilitate the measurement of channel width and depth.

Method one was used to provide a comparison of the results obtained by Method 2. The percentage of silt clay in the channel bed was estimated from examination of thin sections (Chapter 5). The resultant values were 29% for Channels 1 and 2 and 32% for Channel 3. Diagenetic clays could not be distinguished from detrital clays in thin section, thus the above estimates may be too high. The silt-clay content of the channel bank could not be determined but was assumed to be 100% (Nwajide and Hoque, 1984).

The relationships for determining paleohydraulics were developed from modern streams in semi-arid environments. Although the presence of extensive coal seams in the study area indicates a humid environment, the equations may still be applicable because the abundance of vegetation and absence of grasses in the Upper Cretaceous create a hydrologic regime similar to that of present day semi-arid environments (Schumm, 1968).

Channel Width:

The width of a paleochannel (W) can be determined using the horizontal width of the point bar (W^*). Point bars are estimated to extend two-thirds of the way across the width of the channel (Allen, 1965), thus the channel width can be calculated by the following formula:

$$W^* \times 1.5 = W \qquad (1)$$

The true widths of the lateral accretion surfaces in the study area cannot be measured directly from the outcrops due to the orientation of the outcrop face with respect to the actual channel cross section. If the strike of the outcrop face is not perpendicualr to the paleoflow direction, then the width measured will be greater than the actual point bar width.

The following relationship was used to determine the true point bar width:

$$W^{*} = W_{app} \times \cos \theta \qquad (2)$$

where W_{app} is the apparent thickness measured from the outcrop and θ is the angle between the strike of the channel cross section (perpendicular to the paleoflow direction) and the strike of the outcrop face.

Channel Depth:

The paleodepth of the channels can also be determined using the point bar, by measuring the vertical thickness of the lateral accretion unit (Allen, 1965).

In order to estimate the depth, two factors must be taken into account; differences in bankfull depth between straight reaches and meander bends, and compaction resulting from the conversion of sand to sandstone after burial.

The bankfull depth measurements used in the development of the regression equations were taken from the straight reaches of modern rivers. In meandering systems the depth of the channel in the straight reaches is considerably less than at the meander bend. Measurements from Channels 2 and 3 were taken from lateral accretion surfaces which occur at the meander bend, thus a correction factor must be applied. The ratio between straight and meandering bankfull depth has been shown to be 0.585.

To account for the reduction in thickness of the sand body due to the conversion of sand to sandstone, the

thickness of the point bar sandstone must be divided by 0.9 (Chilingarian et al, 1975).

Using the above correction factors the depth of Channels 2 and 3 can be estimated by:

$$\text{Bankfull Channel Depth } (D) = 0.585/0.9\ D^{*} \quad (3)$$

Channel 1 is considered separately since it lacks lateral accretion surfaces. The width of this channel is taken to be the width of the entire sand body and the depth (D) as the maximum thickness of the sand body after the correction for compaction has been made.

For Channel 1:

$$W = W^{*} \quad (4)$$

$$D = D^{*} / 0.9 \quad (5)$$

It should be noted that for Channel 1, corrections for the orientation of the outcrop must also be performed.

Paleohydraulic Calculations:

The percentage of silt-clay in the channel perimeter (M), upon which Method 1 is based, is related to Sb, Sc, W and D by the equation:

$$M = [(Sc \times W)+(Sb \times D)] / (W + 2D) \quad \text{(Schumm, 1960)} \quad (6)$$

The width-depth ratio (F) is obtained by using M or by comparing W and D:

$$F = 255\ M^{-1.08} \qquad \text{METHOD 1} \quad \text{(Schumm, 1960)} \quad (7)$$

$$F = W/D \qquad \text{METHOD 2} \qquad (8)$$

Sinuosity can be calculated by the relationship:

$$P = .94\ M^{.25} \qquad \text{METHOD 1} \quad \text{(Schumm, 1963)} \quad (9)$$

$$P = 3.5\ F^{-2.7} \qquad \text{METHOD 2} \quad \text{(Schumm, 1963)} \quad (10)$$

The mean annual discharge (Qm) is also determined using the parameters F and W according to:

$$Qm^{.38} = W\ M^{.39} / 37 \qquad \text{METHOD 1} \quad \text{(Schumm, 1968)} \quad (11)$$

$$Qm = W^{2.43} / 18\ F^{1.13} \qquad \text{METHOD 2} \quad \text{(Schumm, 1972)} \quad (12)$$

Meander wavelength (L) can be estimated by the equation:

$$L = 1890\ Qm^{.34} / M^{.74} \qquad \text{METHOD 1} \quad \text{(Schumm, 1968)} \quad (13)$$

$$L = 18\ (F^{0.53}\ W^{0.69}) \qquad \text{METHOD 2} \quad \text{(Schumm, 1972)} \quad (14)$$

The percentage of total load as bedload (Bd) is calculated by the equation:

$$Bd = 55 / M \qquad \text{(Schumm, 1968)} \quad (17)$$

It is important to note that the above equations are valid for imperial units only.

Results and Interpretations:

The measured values of W and D for each of the channels are listed in Table 6.1. The results of the paleohydraulic calculations for both Method 1 and Method 2 of Ethridge and Schumm (1978) are found in Table 6.2.

The values for percentage silt-clay in channel perimeter, percentage of total load as bedload, calculated from Method 1, width-depth ratio, and sinuousity for both Mehtod 1 and 2 lie within Schumm's classification for Suspended Load Channels (fig. 6.1). The difference in values between Method 1 and Method 2 may be due to the over-estimation of the value for M, errors in the measurement of channel width and depth, or to imperfections in the formulae.

Sinuosities calculated for all three channels are greater than the value of 1.7 that defines the lower boundary of the highly sinuous and meandering classification (Reineck and Singh, 1980).

Table 6.1 Determined width and depth values for the channels.

TABLE 6.1

CHANNEL	STRIKE OF OUTCROP (deg)	STRIKE OF LATERAL ACCRETION SURFACE (deg)	THETA (deg)	Wapp (m)	W* (m)	W (m)	W (ft)	D* (m)	D (m)	D (ft)
CHANNEL 1	144	81	27	48.9	43.6	43.6	143.0	4.7	5.2	17.1
CHANNEL 2	145	67	11	26.2	25.7	38.6	126.6	4.0	4.4	14.4
CHANNEL 3	124	80	46	10.2	7.1	9.5	31.2	4.6	5.0	16.4

Table 6.2 Results of paleohydraulic calculations for Methods 1 and 2 of Ethridge and Schumm (1978).

TABLE 6.2

CHANNEL		Sb	Sc	M	F	P	Qm (m^3/s)	Qm (ft^3/s)	L (m)	L (ft)	Bd
CHANNEL 1	METHOD 1	100%	29%	42.7%	4.42	2.0	46.7	1650.5	444.6	1458.6	1.30%
	METHOD 2				8.40	2.4	24.5	865.0	120.2	394.4	
CHANNEL 2	METHOD 1	100%	29%	42.3%	4.47	2.0	33.8	1193.5	401.0	1315.5	1.30%
	METHOD 2				8.70	2.4	17.7	623.4	487.4	1599.0	
CHANNEL 3	METHOD 1	100%	32%	67.0%	2.70	2.9	1.3	47.0	95.0	311.7	0.82%
	METHOD 2				1.90	2.7	3.2	113.2	82.3	270.0	

The predicted high sinuosity and meandering nature of the channels is supported by the sand body geometry. The channel sands studied are relatively narrow and isolated and are bounded to the sides by abundant siltstones and mudstones. Highly sinuous fluvial systems are bounded and confined by clay plugs deposited in abandoned meander loops and the back swamp area. The plugs prevent the channel from sweeping across the flood plain and the sand body formed is narrow and elongate. In these systems mudstones tend to be more abundant than sandstones (Walker and Cant, 1984).

Table 6.3 Schumm's Classification of Stable Alluvial Channels (Schumm, 1968).

Sediment Load	Channel Sediment (Percentage of Silt and Clay in Channel Perimeter)	Bedload (Percent of Total Load)	Type of River
Suspended load and dissolved load	>20	<3	Suspended-load channel; width-depth ratio <10; sinuosity >2.0; gradient relatively gentle.
Mixed load	5 to 20	3 to 11	Mixed-load channel; width-depth ratio >10, <40; sinuosity <2.0, >1.3; gradient moderate; can be braided.
Bed load	<5	>11	Bedload channel; width-depth ratio >40; sinuosity <1.3; gradient relatively steep; can be braided.

PALEORECONSTRUCTION:

The positions of the outcrops of Channels 2 and 3 suggest that they were probably part of the same channel.

An attempt at reconstructing the channel morphology was predominantly based on the positions of the outcrops in plan view and the orientation of lateral accretion surfaces and was performed as a comparison for the calculated values of meander wavelength and sinuousity. An aerial view of the outcrops and corresponding paleoreconstruction are included in figs. 6.1 and 6.2..

Results:

The paleoreconstruction of the channel comprised of Channels 2 and 3 indicates a meander wavelength of 420 m. The measured value of sinuosity is defined as the ratio between the down-river length and the down-valley length. In this case, the down-river length is measured as 550 m, giving a sinuosity of 1.4. The meander wavelength measured from the reconstructed version of the channels gives values similar to those calculated for Channel 2 but much higher than those calculated for Channel 3. The measured values of sinuosity are significantly lower than the calculated values.

The differences between calculated and reconstructed values for meander wavelength and sinuosity may be due to an incorrect reconstruction of this portion of the meander belt. Alternatively, differences may be due to the fact

that the portion of the meander belt studied may not be typical of the entire stream. It is common for the size and shape of meanders within a meander belt to vary along the length of the stream.

Figure 6.1 Paleorecostruction of the Channel.

Figure 6.2 Aerial view of outcrop positions.

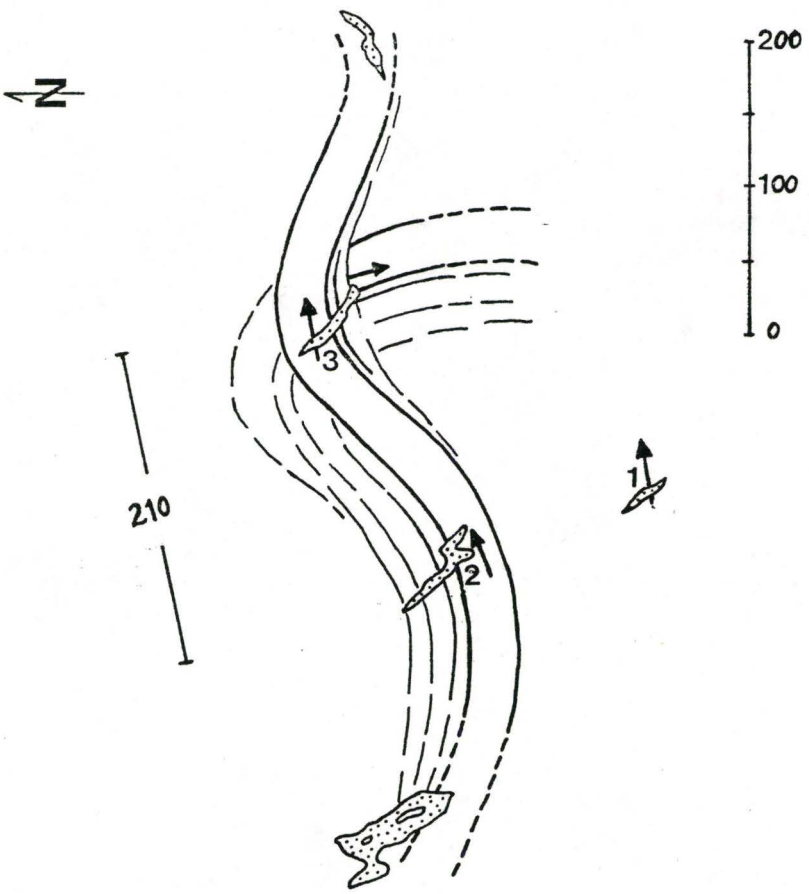
N
200
100
0
210
1
2
3

CHAPTER 7

INTERPRETATIONS AND DISCUSSION

The purpose of this chapter is to integrate the separate facies interpretations into a model for the meandering channel deposits observed in the Drumheller area.

A possible model to explain the sand filling of Channel 1 will be proposed, following the facies interpretations.

Integrated Facies Interpretation:

The strata of the Horseshoe Canyon Formation examined in this study were deposited by a high sinuosity, meandering fluvial system.

The coal which was deposited prior to the fluvial system studied here, existed as peat during the channeling and provided a resistant mat which prevented erosion of the underlying strata by the channels.

Thick, laterally continuous coal seams, such as the seam present in the study area, indicate deposition in a warm, humid environment, possibly that of a flood basin swamp. To prevent decomposition of the peat, the water level must be high enough to keep the peat submerged, but low enough so that peat forming vegetation is not drowned. These conditions are met when the rate of peat formation is

equal to the rate of subsidence (Stach et al., 1975). Protection from eroding currents and clastic input is required for the preservation of the peat, and in the flood basin swamp environment of a channel system, this protection is afforded by the river levees.

The amount of time required for the accumulation of enough peat to form the 2 m thickness of coal observed in the study area can be calculated. Subtropical peats tend to accumulate at a rate of 1 mm per year, and it takes 1 m of peat to yield .2 m of bituminous coal (Stach et al., 1975), thus the coal seam in the study area would require 10 m of peat. Using the estimated accumulation rate, the deposition of Facies 1 would have taken 10,000 years.

The deposition of peat may have ended due to a local change in conditions, resulting in a less humid environment. The presence of the carbonaceous shale, which lies above the coal in Channels 2 and 3, indicates drier conditions and subaerial exposure, which may have occurred as the channel supplying the flood basin migrated farther away.

The active channel deposits of meandering streams overlie, but do not erode into the coals. The three associated deposits which represent the active channel fill are; a channel lag, cross bedded sand with lateral accretion surfaces, and parallel laminated sand.

Lag deposits are present on the channel floor and consist of large clasts which can only move during peak flood periods (Walker and Cant, 1984). The clasts

comprising the lag deposits of the channels studied are tabular and rounded mudclasts and coal clasts.

The tabular mudclasts may represent partially consolidated material eroded from the channel wall. They may have escaped reworking by being deposited below the level of the stream thalweg (Collinson and Thompson, 1982), or by being preserved by rapid burial. Thin, flat mudclasts with preserved internal laminae and evidence of plastic deformation have been attributed to erosion of partially dried, compacted mud that was deposited during a period of low flow (Williams, 1966). The rounded mudclasts may have been derived from the same source as the tabular mudclasts were small enough to undergo transport. It is uncertain if the coal clasts represent ripped up material from the coal, which existed as peat during the time of channeling, or waterlogged plant remains which sank to the channel bottom.

The trough cross bedding and lateral accretion surfaces are characteristic of depostion on the point bar in a meandering fluvial system. The accretion surfaces form by lateral and downstream migration of the point bar in the stream (Allen, 1965). The erosional lower contact which is found below the lag deposit is created in the thalweg of the channel, and as the channel migrates the erosion surface is overlain by point bar deposits (Elliot, 1975). Lateral accretion may have been episodic as indicated by the preservation of sufaces by drapings of "coffee grounds".

Sinuous crested dunes, which are preserved in the form of trough cross bedding, are a bedform typically found on the channel floor. Large scale trough cross-beds have been reported from the lower point bar by Allen (1970). The passing of trough cross bedded sand into ripple cross laminated sand is commonly found in point bar sands. This was not observed, which may have been due to the poor preservation of ripple cross-lamination.

The parallel laminated sand (Facies 6) is always present on the top and sometimes witnin the lateral accretion deposits. Favourable conditions for the formation of parallel lamination can occur both high and low on the point bar (Walker and Cant, 1984). On the upper point bar, flat bedding with parting lineation may occur where increasing flow velocities result from large quantitites of water being forced into confined space (Smith, 1971).

The interfingering brown shale and sand is laterally adjacent to Channel 1 and is interpreted as the proximal overbank deposits of a meandering river. The shales, representing levee deposits, were emplaced along the channel banks when flood waters deposited their sediment load on channel banks.

The interfingering sands are interpreted as crevasse splay deposits which are deposited when the levee is catastrophically breached during flooding. Splay deposits are noted to be similar in grade to channel deposits. The grain size distribution plots (Chapter 4) from this facies

indicate similar grain size distributions for the splay deposits as compared to the channel fill deposits.

The thickness of the crevasse splay deposits indicate that depostion occurred during large flood events. These large floods may have caused major scouring within the channel amd may account for the fact that there appears to be two major events of sand depostion in Channel 1. The lower part of the channel contains a high concentration of "coffee grounds" on the bedding surfaces. An abrupt decrease in the abundance of coffee grounds occurs in the upper half of the channel sand.

The carbonaceous shales occurring at the top of the channel sands are interpreted as vertical accretion deposits, which were emplaced after the channel was abandoned. These deposits were subjected to subaerial exposure as indicated by their reddish colour. The fine grained nature indicates that deposition occurred far from the active channel in an area where stagnant flood waters deposited mud.

The truncation of deposits of Facies 2 and Facies 8 by the channels indicate that the deposition of these units occurred prior to the channeling event studied.

Facies 8 is interpreted as distal overbank deposits and is characterized by the small sand to shale ratio.

Facies 2 appears to represent the point bar deposit of a previous channeling event, since it erosively overlies

Facies B and shows scoured contacts with the overlying channel sands.

The deposits of the channels can be compared to the Meandering River Facies Sequence of Allen (1970), which consists of a channel lag, overlain by cross bedded sands containing ripples and parallel lamination. Above the sands are vertical accretion deposits consisting of fines which were introduced during the flood stage, after the channel had migrated laterally. At least one of the channels studied deviates from Allen's model by containing only a very thin sequence of vertical accretion deposits. Channel 1 appears to be filled to the top with sand. The sand filling of a channel will be discussed on the following pages.

Sand-Filled Meandering Channels:

The sand filling of channels is common in the case of braided channel systems. The sand body geometry and paleohydraulic calcuations suggest a meandering morphology for the channels studied, therefore a mechanism for the sand filling of a meandering channel must be proposed.

Channel 1 is the only channel that clearly shows a sand fill to the top of the channel. Since a portion of the outcrop of Channel 2 has been eroded away, it is not known if this channel is also filled to the top with sand. Channel 3 shows abundant scouring of the upper surface of the sand but also has thick deposits of fines present at the

top of the channel. Only Channel 1 will be considered when discussing sand filled channels.

It is assumed that the channel was filled to the top with sand, and not filled by fines followed by removal of the top of the channel by erosion. This assumption is made due to the lack of evidence of truncation of large scale sedimentary structures by the top of the channel.

Progressive abandonment of a meandering channel is a mechanism by which the channel is filled primarily with bed load sediment followed by a relatively thin sequence of overbank fines.

In order to maintain the flow conditions that allow the transport and deposition of sand within a channel during abandonment, the channel must be abandoned gradually and depth must decrease by aggradation as discharge decreases.

The gradual abandonment of a meander loop can occur by chute cutoff, where a stream shortens its meander loop by cutting a new channel along an old swale. Because of the small angular difference between the two channels, the stream continues to flow through the old channel until the ends are plugged by the depositon of bed load (Allen, 1965). Bed load sediments usually form the main fill of a progressively abandoned channel (Allen, 1965). The channel is then filled to the top with overbank fines.

The absence of any appreciable fine sediment may be due to the erosion of fines during the reoccupation of the old channel at peak flood periods. During high flow periods the

abandoned loop may be reoccupied, removing the previously deposited fines and depositing sand. A series of reoccupation events could result in the removal of fines and the complete sand filling of the channel. The parallel laminated sand may represent a final flood which deposited sand in a shallow stream. A thin layer of vertical accretion deposits was then deposited by overbank flows from the new channel.

Sand-filled meandering channels are not well documented in the geological literature. Fisk (1955) described sand filled channels in the pre- modern Mississippi Delta system and suggested that the filling occured as a result of gradual decrease in flow. In a 1960 paper, he proposed that a gradual decrease in flow could result from the creation and enlargement of a new favoured channel.

Hopkins (1985) described a "U" shaped channel with a symmetrical concave fill of uniform medium sandstone in the Lower Kootenai Formation (Cretaceous). The channels and other surrounding channels are interpreted as suspended load, deltaic distributary channels that formed by avulsion.

The symmetrical concave fill of the channel is attributed to the incremental filling of the channel as a result of a gradual decrease in mean discharge. The progressive abandonment of the distributary is sugested to be a result of the diversion of flow to a different distributary.

It is concluded that the sand filled channel in the Horseshoe Canyon Formation of Drumheller is the result of progressive abandonment of a meander loop by chute cutoff.

Conclusions:

i) Channels in the Upper Horseshoe Canyon Formation of Drumheller, Alberta are interpreted as highly sinuous, suspended load, meandering channels.

ii) The channel sand bodies contain a channel lag overlain by lateral accretion deposits or concave upward surfaces, with trough cross-bedding, ripple cross-lamination and parallel laminated sand. The associated deposits are interpreted as levee, crevasse splay and distal overbank deposits.

iii) Paleoflow directions were generally towards the east.

iv) The sandstones fall within the Lithic Arkose and Feldspathic Litharenite classifications of Folk (1968).

v) The lack of coarse sediments within the channels is dependant on availibility and not the competence of the flow.

vi) Channel 1 filled with sand due to gradual abandonment by chute cutoff. The complete filling with sand may be attributed to episodes of flooding, resulting in the reoccupation of the channel, removal of previously deposited fines and the deposition of sand.

REFERENCES

ALBERTA SOCIETY OF PETROLEUM GEOLOGISTS, 1959. Ninth Annual Field Conference -- Moose Mt.--Drumheller.

ALLEN, J.R.L., 1965. Review of the origin and characteristics of recent alluvial sediments. Sedimentology v.5, p. 89-191.

---------- 1970. Studies in fluviatile sedimentation: a comparison of fining-upward cyclotherms, with special reference to coarse member composition and growth. Jour. Sedimen. Petrol. v.40, p. 298-323.

BASU, A., YOUNG, S.W., SUTTNER, L.J., JAMES, W.C. and MACK, G.H., 1975. Re-evaluation of the use of undulatory extinction and polycrystallinity in detrital quartz for provenance interpretation. Jour. Sedimen. Petrol. v.45, p. 873-882.

BROMLEY, R.G., PEMBERTON S.G.and RAHMANI, R.A., 1984. A Cretaceous Woodground: the Teredolites Ichnofacies: in Trace fossils and paleoenvironments: marine carbonate, marginal marine terrigenous and continental terrigenous settings, Miller, M.F. et al. (eds.), Journal of Paleontology v.58 (2), p. 488-498.

BLATT, H., MIDDLETON, G.V., MURRAY, R., 1980. Origin of Sedimentary Rocks (2nd edn.). Prentice-Hall Inc., New Jersey, U.S.A.

BUURMAN, P., 1975. Possibilities of Paleopedology. Sedimentology v.22 (2), p. 289-298.

CARRIGY, M.A., 1970. Proposed revision of the Boundaries of the Paskapoo formation in the Alberta Plains: Bulletin of Canadian Pertoleum Geology, v.18 (2), p. 156-165.

CHILINGARIAN, G.V., WOLF, K.H., and ALLEN, D.R., 1975. Introduction in G.V. Chilingarian and H.K. Wolf (eds.), Compaction of Coarse Grained Sediments. Elsevier, N.Y., p. 1-42.

COLLINSON, J.D. and THOMPSON, D.B., 1982. Sedimentary Structures. George Allen and Unwin Ltd., London.

DAPPLES, E.C., and HOPKINS, M.E. (eds.), 1969. Environments of Coal Deposition. Geol. Soc. Am. Spec. Paper 114.

ELLIOT,T., 1976. The Morphology, Magnitude and Regime of a Carboniferous Fluvial-Distributary Channel. Jour. Sediment. Petrol., v.46, p. 70-76.

ETHRIDGE, F.G. and SCHUMM, S.A., 1978. Reconstructing paleochannel morphologic and flow characteristics: methodology, limitations and assessment in Miall A.D. (ed), Fluvial Sedimentology, C.S.P.G. Memoir 5, p. 703-722.

FOLK, R.L., 1968. Petrology of Sedimentary Rocks. Hemphill Publishing Co., Austin, Texas. 182 p.

HAYWICK, D.W., 1982. Sedimentology of the Wapiabi-Belly River Transition and the Belly River Formation (Upper Cretaceous) near Ghost Dam, Alberta, in Unpublished B.Sc. Thesis, McMaster.

IRISH, E.J.W., 1967. Drumheller Map-area, Alberta. Geol. Surv. Can., Map 22-1967.

---------- and HAVARD, C.J., 1968. The Whitemud and Battle Formation (Kneehills Tuff Zone) -- a stratigraphic marker. Geol. Surv. Can., Paper 67-63.

---------- 1970. The Edmonton Group of south central Alberta. Bull. Can. Petrol. Geol. v.18 (2), p. 125-155.

LEOPOLD, L.B., and WOLMAN, M.G. 1960. River meanders. Geol. Soc. Am. Bull. v.71, p. 769-794.

LOWE, D.R., 1975. Water escape structures in coarse-grained sediments. Sedimentology v.22, p. 157-204.

McLEAN, J.R. and JERYKIEWICZ, T., 1978. Cyclicity, tectonics and coal: Some aspects of fluvial sedimentology in the Brazeau-Paskapoo Formations, Coal Valley area, Alberta, Canada, in Miall, A.D. (ed.), Fluvial Sedimentology, C.S.P.G. Memoir 5, p. 441-468.

MIALL, A.D., 1981. Analysis of Fluvial Depositional Systems. AAPG Education Course Note Series 20.

MIDDLETON, G.V., 1976. Hydraulic interpretation of sand size distribution. Jour. Geol. v.84, p. 405-426.

---------- and SOUTHARD, J.B., 1977. Mechanics of Sediment Movement. Soc. Ec. Paleon. Min., Tulsa, Oklahoma. 159 p.

MIALL, A.D., 1984. Principles of Sedimentary Basin Analysis. Springer Verlag, New York. 490 p.

MOODY-STUART, M., 1966. High and low sinuosity stream deposits with examples from the Devonian of Spitsbergen. Jour. Sed. Petrol., v.36 (4), p. 1102-1117.

NURKOWSKI, J.R. and RAHMANI, R.A., 1982. An Upper Cretaceous fluvio-lacustrine coal bearing sequence, Red Deer area, Alberta, in Abstracts, IAS Congress, 1982, Hamilton, Ontario. p. 56.

NWIJIDE, C.S. and HOQUE, M., 1984. Paleohydraulic reconstruction of a Late Cretaceous river in the Middle Benue Trough (Nigeria) and its limitations. Palaeogeog., Palaeoclim., Palaeoecol. v.47, p. 245-259.

OBRADOVICH, J.D. and COBBAN, W.A., 1975. A time scale for the Late Cretaceous of the Western Interior of North America. Geol. Assoc. Can., Spec. Pap. No. 13., p. 31-54.

PUIGDEFABREGAS, C., and VAN VLIET, A., 1978. Meandering stream deposits from the Tertiary of the Southern Pyrenees, in Miall, A.D. (ed.), Fluvial Sedimentology, C.S.P.G. Memoir 5, p. 469-485.

RAHMANI, R.A. and LERBEKMO, J.F., 1973. Heavy mineral analysis of Upper Cretaceous and Paleocene sandstones in Alberta and adjacent areas of Saskatchewan, in Caldwell, W.G.E. (ed), The Cretaceous System in the Western Interior of North America, GAC Special Paper #13.

RAHMANI, R.A., 1982. Upper Cretaceous coals in a tidally deposited shoreline sequence: Drumheller, Alberta, in Abstracts: IAS Congress, 1982, McMaster University, Hamilton. p. 58

RAHMANI, R.A., 1982. Mesotidal barrier island sedimentation in the late stages of an Upper Cretaceous marine transgression: Drumheller, Alberta, in Abstracts: IAS Congress, 1982, McMaster University, Hamilton. p. 99.

RAHMANI, R.A., 1983. Facies Relationships and Paleoenvironment of a Late Cretaceous Tide Dominated Delta in Drumheller, Alberta. C.P.S.G. Field Trip Guidebook.

READING, H.G., 1978. Sedimentary Environments and Facies. Elsevier, New York. 357 p.

SCHUMM, S.A., 1960. The shape of alluvial channels in relation to sediment type. U.S.G.S. Prof. Paper 352 B. 30 p.

----------1963. Sinuosity of Alluvial Rivers on the Great Plains. Geol. Society America Bulletin v.74, p.1089-1100.

----------1968. Speculations concerning paleohydraulic controls of terrestrial sedimentation. Bull. Geol. Soc. Am. v.79, p. 1573-1588.

----------1972. Fluvial paleochannels in J.K. Rigby and W.K. Hamblin,(eds.), Recognition of Ancient Sedimentary Environments. Soc. Ec. Paleon. Min., Spec. Pub. 16, p. 98-107.

SHEPHEARD, W.W. and HILL, L.V., 1970. Depositional Environments, Bearpaw Horseshoe Canyon (Upper K) transition zone, Drumheller "Badlands", Alberta. Bulletin Canadian Petroleum Geology vol 18, no. 2, pp. 166-215

SMITH, N.D., 1971. Pseudo-planar stratification produced by very low amplitude sand waves. Jour. Sedim. Petrol. v.41, p. 69-73.

STACH, E., MARKOWSKY, M.-TH., TEICHMULLER, M., TAYLOR, G.H., CHANDRA, D. and TEICHMULLER, R., 1975. Stach's Textbook of Coal Petrology, 2nd ed., Gebruder Borntraeger, Berlin.

STEWART, D.J., 1981. A meander belt sandstone of the Lower Cretaceous of Southern England. Sedimentology v.28 (1), p. 1-20.

---------- 1983. Possible suspended load channel deposits from the Wealden Group (Lower Cretaceous), Southern England. Spec. Pub. Int. Assoc. Sedimen. 6, p. 369-389.

TOZER, E.T., 1956. Upper Cretaceous and Paleocene non-marine molluscan faunas of Western Alberta. Geol. Surv. Can., Memoir 280.

WAHEED, A., 1983. Sedimentology of the coal-bearing Bearpaw -- Horseshoe Canyon Formation (Upper Cretaceous), Drumheller area, Alberta, Canada. Master's Thesis, Univ. of Toronto, Toronto, Ontario, Canada.

WALKER, R.G. and CANT, D.J., 1984. Sandy Fluvial Systems, in Walker, R.G. (ed.), Facies Models (2nd edn.), Geoscience Canada Reprint Series 1.

WILLIAMS, G.D. and BURK, C.F.Jr., 1964. Upper Cretaceous, in McCrossan, R.G. and Glaister, R.P., (eds.), Geological History of Western Canada. Alta. Soc. Petrol. Geol., Calgary, p. 169-189.

WILLIAMS, G.D., 1966. Origin of Shale-Pebble Conglomerate. Bulletin A.A.P.G. v.50, p. 573-577.

WILLIAMS, G.D. and STELCK, C.R., 1975. Speculations on the Cretaceous Paleogeography of North America, in W.G.E. Caldwell (ed.), The Cretaceous System in the Western Interior of North America. Geological Association of Canada Special Paper No. 13, p. 1-20.

APPENDIX A

GRAIN SIZE ANALYSIS SIEVING METHOD

(1) Rock samples of approximately 10 grams were weighed prior to disaggregation.

(2) The samples were noted to be weakly cemented by carbonate and were disaggregated using a 2% HCl solution.

(3) In order to deflocculate the clay sized fraction, 500 mls of distilled water and approximately 5 gms of Calgon were added to each sample.

(4) The samples were washed using distilled water through a 40 sieve to remove the fine fraction. Attempts were made to retain the fines by filtering the water through a fine filter but the abundance of fines clogged the filters almost immediately and made filtering impossible.

(5) The dried sand samples were weighed.

(6) Each sample was dry sieved using a half phi size difference beween sieves. The sieving was performed using a mechanical sieve shaker.

(7) Each fraction was carefully removed from the sieves and weighed.